SUPPORTING INFORMATION

SI Materials and Methods

Study subjects. Plasma samples were obtained for seven chronically HIV-1 infected transmitting donors and eight matched acutely infected recipients enrolled in the CHAVI-001 acute and established HIV-1 infection cohorts (1). A summary of available epidemiological, clinical and infection status data is shown in Table S1. In all but one case, acutely infected individuals were identified first and staged using the Fiebig classification (2), while the transmitting partners were identified retrospectively. Epidemiological linkage was confirmed through viral sequence analysis, which also indicated considerable quasispecies diversity in all transmitting donors except CH1064, who may have transmitted during earlier stages of infection (Fig. S1). Transmission pairs were selected based on the following criteria: (i) high transmitting donor plasma viral loads (generally >100,000 vRNA copies/ml) to increase the likelihood of obtaining virus isolates, (ii) availability of donor genital secretions within a year following transmission, (iii) single transmitted founder infections of the recipients to ensure a stringent mucosal bottleneck (one recipient was subsequently found to harbor two transmitted founder viruses), and (iv) absence of antiretroviral treatment. Whole blood was collected in acid citrate dextrose, and plasma was separated and stored at −80°C. In addition, cell-free fractions of genital secretions (GS) were obtained from five of the seven donors. Ectocervicovaginal lavage (CVL) was performed on non-menstruating women using 10 ml of phosphate buffered saline (PBS). Semen ejaculate was collected in 2.5ml of transport medium (RPMI 1640, 1,000 U/ml penicillin, 1 mg/ml streptomycin, 200U/ml nystatin). Genital secretion samples were centrifuged for 10 min at 800g to pellet cells; supernatants were harvested, aliquoted and stored at -80˚C. Written informed consent

was obtained from each subject and the study was approved by the Institutional Review Boards of the University of Pennsylvania and Duke University.

Human CD4+ T-cell isolation and activation. CD4+ T-cells were positively selected from buffy coats of normal subjects (Research Blood Component, Boston, MA or ZenBio Inc., Research Triangle Park, NC) using Human CD4 Microbeads (Miltenyi Biotec Inc., San Diego, CA), viably frozen in CryoStor® CS5 medium (Sigma-Aldrich, St Louis, MO), and stored in liquid nitrogen. Cell aliquots were thawed quickly in a 37°C water bath, resuspended at a density of 2×10^6 cells/ml, and allowed to recover overnight in RPMI 1640 medium containing 15% (vol/vol) fetal bovine serum (FBS) and 30 IU/mL interleukin-2 (IL-2) (CD4+ T-cell medium) in a 37°C incubator with 5% (vol/vol) CO_2. Cells were stimulated using the Human T Cell Activation/Expansion Kit (Miltenyi Biotec Inc., San Diego, CA) and expanded for 4-5 days in CD4+ T-cell medium following the manufacturer's protocol.

Interferons and cytokines. IFNα2 was purchased from PBL Assay Science (Piscataway, NJ). IFNβ was purchased from PBL Assay Science and EMD Serono USA (Rebif®, EMD Serono Inc., Rockland, MD). Interleukin-2 was purchased from the Hospital of the University of Pennsylvania pharmacy (Aldesleukin).

Virus quantification. Viral stocks were characterized by determining their reverse transcriptase (RT) activity using the colorimetric Reverse Transcriptase Assay (Sigma-Aldrich, St Louis, MO), and their p24 antigen content was determined using the HIV p24 (high sensitivity) AlphaLISA Detection Kit (Perkin Elmer Inc., Boston, MA).

Generation of limiting dilution-derived HIV-1 isolates. To generate limiting dilution-derived viral isolates, plasma samples were end-point diluted and used to infect activated normal donor CD4+ T-cells in 24 well plates such that no more than 30% of wells became p24 antigen positive. Assuming that approximately one virus per 1,000 particles is infectious, we started with ~500 vRNA copies/well. Plasma aliquots containing ~12,500 vRNA copies were diluted in 1ml of CD4+ T-cell medium containing 50µl of HIV Infectivity Enhancement Reagent (Miltenyi Biotec Inc., San Diego, CA). To allow the formation of HIV-1 enhancement complexes, tubes were placed on a MACSmix Tubes Rotator (Miltenyi Biotec Inc., San Diego, CA) and incubated at 4˚C under constant rotation at 4 rpm for 30 min. Activated CD4+ T-cells were seeded ($1x10^6$ per well) in a 24-well plate in 500µl of fresh CD4+ T-cell medium; 40µl of the complex-containing solution were added to each well (500 vRNA copies/well), incubated for 12-16 hours in a 37°C incubator with 5% (vol/vol) CO_2, and then supplemented with an additional 1ml of T-cell medium. At days 5, 10 and 15, activated CD4+ T-cells ($1x10^6$ in 500µl of T-cell medium) were added to each well to provide new target cells for virus replication. At day 20, p24 positive wells were identified using the HIV p24 (high sensitivity) AlphaLISA detection kit (Perkin Elmer Inc., Boston, MA). For some plasma samples the number of vRNA copies per well had to be adjusted to reach limiting-dilution conditions. These values ranged between 3 vRNA copies/well (CH831) to 2,000 vRNA copies/well (CH040), indicating a wide range of per particle infectivity, including in acute infection plasmas.

Low viral loads in plasma samples from subjects CH162, CH728 and CH302 (Table S1) required larger volumes of plasma to reach the target dose of 500 vRNA copies per well. These larger volumes decreased cell viability during the first incubation step of the isolation procedure. We thus purified the same amount of virus particles from these samples prior to infection using the µMACS VitalVirus HIV Isolation Kit (Miltenyi

Biotec Inc., San Diego, CA). Virus-microbead complexes were eluted from µ-Columns in 1ml of T-cell medium and 40µl were added to each well (500 vRNA copies/well) of activated target T-cells as described above.

To generate IFN resistant virus isolates, activated CD4+ T-cells were pre-treated with 4.0 pg/ml of IFNα2 or 44 ng/ml of IFNβ for 24 hours prior to isolation with no further addition of IFN. The rationale was to maximally upregulate antiviral ISGs in these target cells, but to then isolate virus in the absence of interferon. For IFNβ, we were able to use a selection dose that was six orders of magnitude higher than the average IFNβ IC_{50} value of all isolates. However, this was not possible for IFNα2 since doses higher than 5.5 pg/ml caused toxicity in the culture. Thus, IFNα2 pretreatment was kept at 4.0 pg/ml. Following treatment, cells were washed once in T-cell medium before being plated in 24-well plates as described above.

For virus isolation from CVL and semen samples, aliquots were thawed at room temperature, fetal bovine serum was added to a final concentration of 2%, and virus isolation was performed as described above. Since virus load information was not available, 1ml aliquots were used per well for one 24-well isolation plate. To inhibit the growth of bacteria, yeast and fungi, T-cell medium was supplemented with penicillin (100 units/ml), streptomycin (100 µg/ml), and Amphotericin B (0.25 µg/ml) (Gibco® Antibiotic-Antimycotic, ThermoFisher Scientific, Waltham, MA). While isolation attempts from all plasma samples were successful, the efficiency of isolation from genital secretion samples was variable: only 1 of 4 CVL samples from donor CH492, 1 of 2 CVL samples from donor CH596, and 4 of 5 semen samples from donor CH742 yielded isolates (Table S1). In contrast, none of 4 CVL and semen samples from donors CH1064 and CH728, respectively, yielded isolates (Table S1).

Virus stock preparation and genotyping. Cells and supernatants from p24 positive wells were transferred to T25 flasks containing $10x10^6$ activated T-cells in 10ml of fresh T-cell medium. After 5 days of culture, an additional $10x10^6$ activated T-cells in 10ml of fresh T-cell medium were added to each flask. At day 10 post-infection, virus-containing supernatant was passed through a 0.45μm nylon membrane syringe filter (Corning, NY) and stored in aliquots at -80˚C.

To sequence each expanded virus isolate prior to its biological characterization, viral RNA was extracted from 100μl of culture supernatant, reverse-transcribed using SuperScript III Reverse Transcriptase (ThermoFisher Scientific, Waltham, MA) and previously published primers (3, 4), and the resulting cDNA was used to amplify overlapping 5' and 3' genome halves in separate triplicate PCR reactions as described (3-5). Ten nanograms (1μl of a 1/25 dilution of the PCR reaction) of each of the 5' and 3' amplicons were then pooled and sequenced using an Illumina NGS platform. DNA libraries were prepared using the Nextera DNA Library Preparation Kit (Illumina Inc, San Diego, CA), as previously described (6, 7) with minor modifications. Briefly, amplicons were fragmented using Nextera tagmentation buffers TD and TDE1 in a final volume of 2.5μl. The tagmentation reaction was subjected to two rounds of PCR amplification using the KAPA Library Amplification Kit (Kapa Biosystems Inc., Wilmington, MA). The first round of PCR incorporated Index 1 (N7xx) and Index 2 (S5xx) adapters (final volume 7.5μl; 98°C for 3 min followed by 8 cycles, 98°C for 15 sec, 62°C for 30 sec, 72°C for 1.5 min); the second round of PCR (final volume 17μl; 95°C for 5 min followed by 7 cycles, 98°C for 20 sec, 62°C for 20 sec, 72°C for 30 sec) was performed with the Nextera adapter primers P1 (5'-AATGATACGGCGACCACCGA-3') and P2 (5'-CAAGCAGAAGACGGCATACGA-3') to enrich the library for tagmented fragments containing the Index 1-Index 2 adapter combination at their ends. DNA libraries were prepared in 96-well plates. Agencourt AMPure XP beads (Beckman Coulter Inc.,

Indianapolis, IN) were used to purify PCR amplicons and to size select ~300bp fragments; eight PCR reactions from each column were combined into a single tube and incubated with 136µl of AMPure XP beads for 5 min at room temperature. Beads were washed thrice with 70% ethanol, air-dried for 5 min, and the bound DNA was eluted in 100µl of 10mM Tris-HCl (pH 8.0). Eluted DNA from all 96 wells were pooled and quantified using Qubit (ThermoFisher Scientific, Waltham, MA) and the Agilent DNA 1000 Kit on a 2200 TapeStation instrument (Agilent Technologies, Santa Clara, CA) to determine the molar concentration of the ~300bp fragments. The pooled library was then diluted to a concentration of 4nM in 10mM Tris-HCl (pH 8.0) and stored at -20˚C until sequencing. Sequencing was performed using Illumina MiSeq or MiniSeq instruments (Illumina Inc, San Diego, CA). Libraries containing 96 samples were run using Illumina MiSeq Nano Kit v2 300. Libraries containing 192 samples were run using Illumina MiSeq Micro Kit v2 300 or Illumina MiniSeq Mid Output Kit 300 (Illumina Inc., San Diego, CA).

All reads were trimmed of adapter sequences, and paired-end reads were combined into a single file, binned for each sample based on index sequences, and assembled to a subtype-matched HIV-1 reference genome using the Cutadapt and SPAdes genome assembler utilities (8, 9). Contigs that aligned to the HIV-1 reference sequence were then used to generate a new sample-specific consensus sequence using reads from triplicate amplifications. Reads were then re-aligned to this sample-matched reference to generate a final full-length isolate consensus sequence using Geneious 9.0 (10). Each nucleotide position of this consensus sequence was inspected for the presence of mixed bases, and isolates that exhibited more than 15% diversity at any one position in the alignment were considered to contain more than one variant and removed from further analysis.

Particle Env content. 250µl aliquots of viral stocks were depleted of microvesicles using magnetic beads coated with anti-CD45 antibody (ThermoFisher Scientific, Waltham, MA). Virions were then isolated from the microvesicle-depleted supernatants using the VitalVirus HIV Isolation kit (Miltenyi Biotec Inc., San Diego, CA) and lysed to release viral proteins. The amount of particle-associated reverse transcriptase activity was determined using a colorimetric Reverse Transcriptase Assay (Sigma-Aldrich, St Louis, MO). Particle-associated Env content was determined using an in-house quantitative ELISA. 96-well plates were coated with 200ng of eCD4-Ig (11) in 100µl of 0.2M sodium carbonate/bicarbonate buffer overnight at 4°C. Wells were washed twice with 200µl of PBS containing 0.2% Tween 20 (PBS-T), blocked at room temperature for two hours with 200µl of 5% milk in PBS-T, and washed three times with PBS-T. 100µl of virus lysate was added per well and incubated at 37°C for two hours. After washing wells five times with PBS-T, 100µl of polyclonal human anti-gp120 conjugated to horseradish peroxidase (ABL Inc., Rockville, MD) was added for one hour at 37°C. Wells were again washed five times with PBS-T, incubated with 100µl o-phenylenediamine dihydrochloride substrate (ThermoFisher Scientific, Waltham, MA) at room temperature for 30 minutes, and then absorbance was read at 450nm. Env content was calculated using a standard curve of recombinant gp120 (10ng to 125pg in 2-fold dilutions), which was then normalized by reverse transcriptase activity. Stocks previously characterized by a similar protocol (12), as well as viral stocks independently quantified for Env content (13), were used to validate the Env ELISA ($r = 0.82$, $P < 0.0001$).

Analysis of per-particle infectivity. Individual wells of a 96-well plate were seeded with 8.3×10^3 TZM-bl cells in 100µl of 10% FBS-containing DMEM medium to achieve ~30% confluence. 24 hours later, cells were infected with 100µl of virus, diluted serially in 10% DMEM with 80µg/ml DEAE dextran. 12-15 hours post-infection, the T-1249 fusion

inhibitor was added (0.01 mg/ml) to prevent multiple rounds of infection. Infections were terminated at 48 hours and cells were lysed in 75µl lysis buffer (Promega Life Sciences, Madison, WI). Relative light units (RLU) generated per volume of each viral stock were calculated by averaging all virus dilutions in the linear range of the assay ($1.5x10^3$ - $7x10^4$ RLUs). The infectivity per particle was then calculated as the RLU generated per pg of RT activity present in each virus stock.

Replicative capacity and type I IFN resistance. Activated normal donor CD4+ T cells were left untreated or cultured in the presence increasing amounts of IFNα2 (0.00074 pg/ml - 5.5 pg/ml) or IFNβ (0.000067 pg/ml - 0.44 pg/ml) for 24 hours. Cells were washed, and $1x10^6$ cells were infected overnight with an equivalent amount of each virus (1ng RT activity). Supernatants were sampled every 48 hours, and cultures were maintained for 7 days while replenishing IFN-containing medium. Virus replication was measured for each IFN concentration as the amount of p24 produced at day 7 and plotted as the percentage of viral growth in the absence of IFN, which was set to 100%. This allowed us to determine the IFNα2 and IFNβ concentrations required to inhibit virus replication by 50% (IC_{50}) as well as the residual virus replicative capacity (Vres) in the presence of maximal IFNα2 and IFNβ concentrations. The replicative capacity of each virus isolate was calculated using p24 antigen levels in untreated cells. Some viruses replicated to titers below the limit of detection in the presence of maximal IFNβ concentrations. For these viruses, the limit of detection (0.1 ng of p24/ml) was used as the numerator to calculate Vres. IFNα2 IC_{50} values were determined using pooled CD4+ T-cells from 4 donors, while IFNβ IC_{50} values were determined using pooled CD4+ T-cells from 3 donors (Fig. 2A and B). All viruses were tested in duplicate.

Quantification of virus release. CD4+ T-cells were infected as described above. To quantify cell-associated p24, cells and supernatant were harvested 7 days post-infection after centrifugation at 1,200 rpm for 5 min. Cells were lysed, and cell-free and cell-associated p24 antigen levels were quantified using the HIV p24 (high sensitivity) AlphaLISA Detection Kit (Perkin Elmer Inc., Boston, MA). For each isolate, total p24 production was calculated by adding cell-free and cell-associated p24 levels. The percent of released p24 was determined by dividing the cell-free amount of p24 by the total amount of p24 as previously described (14, 15).

Phylogenetic analyses. Nucleotide sequences were aligned using CLUSTALW v. 2 (16). Regions that could not be unambiguously aligned were removed. Maximum likelihood trees with bootstrap support (1,000 replicates) were constructed using PhyML v. 3.1 (17) with evolutionary models selected using jModelTest v. 2.1.4 (18, 19), or for larger datasets, RAxML using a GTRGAMMA model (20). Transmitted founder viral genomes were inferred as described previously (5). Highlighter plots were generated using the Los Alamos National Laboratory HIV Sequence Database Highlighter Tool (https://www.hiv.lanl.gov/content/sequence/HIGHLIGHT/highlighter_top.html). The degree of phylogenetic association of sequences was quantified by calculating their genealogical sorting index (gsi) (21). Maximum likelihood phylogenies were inferred using PhyML (17) and multiple bifurcations with intervening zero-length branches were collapsed to polytomies using the di2multi method implemented in the ape package (22) of R (23). These phylogram topologies were used to calculate the gsi values; p-values were determined using 10,000 replicate permutations (21).

Statistical analyses. For intra-pair comparisons of viral properties, p-values were determined using Welch's unequal variances t-test. Analyses were performed in R (23),

comparing log_{10}-transformed values for matched donor and recipient isolates for each transmission pair. Some isolates had undetectable p24 values after treatment with IFNβ. Since the unmeasurable range of p24 antigen (0 to 0.1 ng/ml) was negligible in comparison to the measurable range (0.1 to 150 ng/ml), a value of 0.1 ng/ml was used as the numerator for calculating IFNβ Vres values. Principal component and receiver operating characteristic analysis (24) were performed using R v3.3.1 (23).

Bayesian hierarchical regression models of viral properties. Each viral property, was modeled using a Bayesian hierarchical model (25), which was based on a linear regression estimating the differences between donor plasma and genital secretion isolates, or donor plasma and recipient plasma isolates, along with the effects of HIV-1 subtype, and IFNα2 and IFNβ-selection. Unlike a normal linear regression, this model accounts for (i) nested measurements within transmission pairs, (ii) multiple transmissions from a single donor, (iii) heteroscedasticity among virus populations, and (iv) censored data where exact measurements were not available but known to be less than a given value. The hierarchical models are based on the assumption that observations of viral properties are independent and identically normally distributed with mean and variance drawn from common population-level distributions. Estimates of the population-level distributions can then be used to infer broader patterns in the data.

Data were first transformed as follows:

Variable	Transformation
Env/RT	log
Infectivity	log
Replicative capacity	log
IFNα2 IC_{50}	log
IFNβ IC_{50}	log
IFNα2 Vres	logit
IFNβ Vres	logit
p24 antigen release	logit

The observation from each viral isolate i was then modeled as a normal distribution $N(\mu_i, \sigma_i^2)$ with mean μ_i:

$$\begin{aligned}\mu_i = \; & \text{donor}_{\text{pair}_i} \\ & + \beta_{\text{recipient,pair}_i} \mathbb{1}(\text{recipient}_i) \\ & + \beta_{\text{genital,pair}_i} \mathbb{1}(\text{genital}_i) \\ & + \beta_{\text{clade,pair}_i} \mathbb{1}(\text{cladeB}_i) \mathbb{1}(\text{recipient}_i) \\ & + \beta_{\text{donorAlpha,pair}_i} \mathbb{1}(\text{donor}_i \;\&\; \text{alphaSelect}_i) \\ & + \beta_{\text{donorBeta,pair}_i} \mathbb{1}(\text{donor}_i \;\&\; \text{betaSelect}_i) \\ & + \beta_{\text{recipientAlpha,pair}_i} \mathbb{1}(\text{recipient}_i \;\&\; \text{alphaSelect}_i) \\ & + \beta_{\text{recipientBeta,pair}_i} \mathbb{1}(\text{recipient}_i \;\&\; \text{betaSelect}_i)\end{aligned}$$

and variance σ_i^2:

$$\sigma_i^2 = \begin{cases} \sigma^2_{\text{genital,pair}_i} & \text{if genital}_i \\ \sigma^2_{\text{recipient,pair}_i} & \text{if recipient}_i \\ \sigma^2_{\text{donorAlpha,pair}_i} & \text{if donor}_i \;\&\; \text{alphaSelect}_i \\ \sigma^2_{\text{donorBeta,pair}_i} & \text{if donor}_i \;\&\; \text{betaSelect}_i \\ \sigma^2_{\text{donor,pair}_i} & \text{otherwise} \end{cases}$$

where pair $_i$ indicates the pair identity of the i^{th} observation, donor_j is the estimated mean of untreated donor plasma viral isolates from pair j and $1\,()$ is an indicator function that is 1 if True and 0 if False. The various β values are coefficients modeling the change expected for viruses in recipients, in donor genital samples, in recipients infected with

HIV-1 clade B, and the effects of IFNα2 and IFNβ-selection on donor or recipient viruses. For example, a donor plasma virus i from pair 2 would have mean $\mu_i = \text{donor}_2$ and an IFNα2-selected recipient virus from pair 3 (which happened to be clade B) would have mean:

$$\mu_i = \text{donor}_3 + \beta_{\text{recipient},3} + \beta_{\text{clade},3} + \beta_{\text{recipientAlpha},3}$$

For two transmission pairs where one donor (CH742) transmitted viruses to two separate recipients (CH378 and CH831), recipient parameters were estimated independently for each recipient.

Vres measurements were calculated as the amount of p24 released in the presence of the highest IFN dose divided by the released p24 without IFN treatment as measured by AlphaLISA. The limit of detection for these measurements was 0.1, so concentrations ≤ 0.1 were measured as 0.1. To account for this, the probability of these observations was considered to be:

$$p\left(\text{Vres} = \frac{0.1}{\text{Untreated p24}}\right) = \int_{-\infty}^{\text{logit}\left(\frac{0.1}{\text{Untreated p24}}\right)} N(\mu_i, \sigma_i^2)$$

The coefficients β for each pair j come from population-level normal hyperpriors:

$$\begin{aligned}
\text{donor}_j &\sim N(\mu_{\text{donor}}, \sigma^2_{\text{donor}}) \\
\beta_{\text{recipient},j} &\sim N(\mu_{\text{recipient}}, \sigma^2_{\text{recipient}}) \\
\beta_{\text{genital},j} &\sim N(\mu_{\text{genital}}, \sigma^2_{\text{genital}}) \\
\beta_{\text{clade},j} &\sim N(\mu_{\text{clade}}, \sigma^2_{\text{clade}}) \\
\beta_{\text{donorAlpha},j} &\sim N(\mu_{\text{donorAlpha}}, \sigma^2_{\text{donorAlpha}}) \\
\beta_{\text{donorBeta},j} &\sim N(\mu_{\text{donorBeta}}, \sigma^2_{\text{donorBeta}}) \\
\beta_{\text{recipientAlpha},j} &\sim N(\mu_{\text{recipientAlpha}}, \sigma^2_{\text{recipientAlpha}}) \\
\beta_{\text{recipientBeta},j} &\sim N(\mu_{\text{recipientBeta}}, \sigma^2_{\text{recipientBeta}})
\end{aligned}$$

and coefficients σ from population-level normal hyperpriors:

$$\sigma_{\text{donor},j} \sim N(\theta_{\text{donor}}, \phi^2_{\text{donor}})$$
$$\sigma_{\text{donorAlpha},j} \sim N(\theta_{\text{donorAlpha}}, \phi^2_{\text{donorAlpha}})$$
$$\sigma_{\text{donorBeta},j} \sim N(\theta_{\text{donorBeta}}, \phi^2_{\text{donorBeta}})$$
$$\sigma_{\text{recipient},j} \sim N(\theta_{\text{recipient}}, \phi^2_{\text{recipient}})$$
$$\sigma_{\text{genital},j} \sim N(\theta_{\text{genital}}, \phi^2_{\text{genital}})$$

The effect hyperparameters $\mu_{\text{recipient}}$, μ_{genital}, μ_{clade}, $\mu_{\text{donorAlpha}}$, $\mu_{\text{donorBeta}}$, $\mu_{\text{recipientAlpha}}$ and $\mu_{\text{recipientBeta}}$ were all given a flat prior probability. The variance parameters σ_{donor}, $\sigma_{\text{recipient}}$, σ_{genital}, σ_{clade}, $\sigma_{\text{donorAlpha}}$, $\sigma_{\text{donorBeta}}$, $\sigma_{\text{recipientAlpha}}$, $\sigma_{\text{recipientBeta}}$, ϕ_{donor}, $\phi_{\text{donorAlpha}}$, $\phi_{\text{donorBeta}}$, $\phi_{\text{recipient}}$, ϕ_{genital}, θ_{donor}, $\theta_{\text{donorAlpha}}$, $\theta_{\text{donorBeta}}$, $\theta_{\text{recipient}}$ and θ_{genital} were given a prior of Gamma (1,2) reflecting prior knowledge that the standard deviation in these assays was unlikely to be greater than several logs.

Plots and statistics are based on the estimated posterior probabilities of the population-level effects $\mu_{\text{recipient}}$, μ_{genital}, μ_{clade}, $\mu_{\text{donorAlpha}}$, $\mu_{\text{donorBeta}}$, $\mu_{\text{recipientAlpha}}$ and $\mu_{\text{recipientBeta}}$. Markov Chain Monte Carlo sampling of the posterior probability distributions of the models was implemented in Stan (26) using the R package rstan (23) and run in 50 chains with each having a 50,000 iteration burn-in and 50,000 iterations of sampling every 25$^{\text{th}}$ iteration.

Biological data and analysis code are archived on Zenodo at:

DOI: 10.5281/zenodo.21645

As an example for why these Bayesian estimates are more conservative than simpler analyses, we can look at the estimated change in IFNβ IC_{50} between untreated donor plasma viruses and IFNβ-selected donor plasma viruses (Fig. 3). We observed $\log_{10}(IC_{50})$ in both untreated and IFNβ-selected viral isolates for 3 donors with averages:

Donor	Untreated	IFNβ-selected	Difference
CH148	-4.269	-2.831	1.438
CH492	-4.203	-2.717	1.487
CH596	-4.162	-2.820	1.343

The simplest estimate would be to take the average, 1.423, and the standard deviation, 0.0733, of the three differences and estimate the 95% confidence interval on the mean as:

$$1.423 \pm \frac{1.96 \times 0.0733}{\sqrt{3}} = 1.423 \pm 0.0829$$

Or equivalently an estimate that IFNβ-selected donor viruses have an IC_{50} 26.5-fold (95% confidence interval: 21.9–32.0-fold) higher than untreated isolates. In contrast, the Bayesian model yielded estimates of 20.7-fold (95% credible interval: 11.0–36.2-fold) higher IC_{50} values. Thus, the Bayesian model represents a more conservative approach that yields wider intervals in its estimation due to the incorporation of uncertainty in our estimates of untreated and IFNβ-selected IC_{50} values for each donor.

SI References

1. Cope AB, et al. (2015) Ongoing HIV transmission and the HIV care continuum in North Carolina. *PLoS One* 10(6):e0127950.
2. Fiebig EW, et al. (2003) Dynamics of HIV viremia and antibody seroconversion in plasma donors: implications for diagnosis and staging of primary HIV infection. *AIDS* 17(13):1871-1879.
3. Salazar-Gonzalez JF, et al. (2008) Deciphering human immunodeficiency virus type 1 transmission and early envelope diversification by single-genome amplification and sequencing. *J Virol* 82(8):3952-3970.
4. Salazar-Gonzalez JF, et al. (2009) Genetic identity, biological phenotype, and evolutionary pathways of transmitted/founder viruses in acute and early HIV-1 infection. *J Exp Med* 206(6):1273-1289.
5. Keele BF, et al. (2008) Identification and characterization of transmitted and early founder virus envelopes in primary HIV-1 infection. *Proc Natl Acad Sci USA* 105(21):7552-7557.
6. Kryazhimskiy S, Rice DP, Jerison ER, & Desai MM (2014) Microbial evolution. Global epistasis makes adaptation predictable despite sequence-level stochasticity. *Science* 344(6191):1519-1522.
7. Baym M, et al. (2015) Inexpensive multiplexed library preparation for megabase-sized genomes. *PLoS One* 10(5):e0128036.
8. Martin M (2011) Cutadapt removes adapter sequences from high-throughput sequencing reads. *Embnet.Journal doi:10.14806/ej.17.1.200* 17(1).
9. Bankevich A, et al. (2012) SPAdes: a new genome assembly algorithm and its applications to single-cell sequencing. *J Comput Biol* 19(5):455-477.

10. Kearse M, et al. (2012) Geneious Basic: an integrated and extendable desktop software platform for the organization and analysis of sequence data. *Bioinformatics* 28(12):1647-1649.
11. Gardner MR, et al. (2015) AAV-expressed eCD4-Ig provides durable protection from multiple SHIV challenges. *Nature* 519(7541):87-91.
12. Parrish NF, et al. (2013) Phenotypic properties of transmitted founder HIV-1. *Proc Natl Acad Sci USA* 110(17):6626-6633.
13. Chertova E, et al. (2002) Envelope glycoprotein incorporation, not shedding of surface envelope glycoprotein (gp120/SU), Is the primary determinant of SU content of purified human immunodeficiency virus type 1 and simian immunodeficiency virus. *J Virol* 76(11):5315-5325.
14. Kluge SF, et al. (2014) Nef proteins of epidemic HIV-1 group O strains antagonize human tetherin. *Cell Host Microbe* 16(5):639-650.
15. Kmiec D, et al. (2016) Vpu-Mediated counteraction of tetherin is a major determinant of HIV-1 interferon resistance. *MBio* 7(4):e00934-00916.
16. Larkin MA, et al. (2007) Clustal W and Clustal X version 2.0. *Bioinformatics* 23(21):2947-2948.
17. Guindon S, et al. (2010) New algorithms and methods to estimate maximum-likelihood phylogenies: assessing the performance of PhyML 3.0. *Syst Biol* 59(3):307-321.
18. Hurvich CM & Tsai CL (1995) Model selection for extended quasi-likelihood models in small samples. *Biometrics* 51(3):1077-1084.
19. Darriba D, Taboada GL, Doallo R, & Posada D (2012) jModelTest 2: more models, new heuristics and parallel computing. *Nat Methods* 9(8):772.
20. Stamatakis A (2014) RAxML version 8: a tool for phylogenetic analysis and post-analysis of large phylogenies. *Bioinformatics* 30(9):1312-1313.

21. Cummings MP, Neel MC, & Shaw KL (2008) A genealogical approach to quantifying lineage divergence. *Evolution* 62(9):2411-2422.

22. Paradis E, Claude J, & Strimmer K (2004) APE: Analyses of phylogenetics and evolution in R language. *Bioinformatics* 20(2):289-290.

23. R Core Team (2016) A language and environment for statistical computing. R Foundation for Statistical Computing, Vienna, Austria. https://www.R-project.org/ [accessed December 21, 2016].

24. Robin X, et al. (2011) pROC: an open-source package for R and S+ to analyze and compare ROC curves. *BMC Bioinformatics* 12:77.

25. Gelman A, Carlin J, Stern H, & Rubin D (2003) Bayesian Data Analysis, Second Edition. Chapman & Hall/CRC, New York, NY.

26. Carpenter B, et al. (In press) Stan: A probabilistic programming language *J Stat Softw.*

27. Bonsignori M, et al. (In press) Staged induction of HIV-1 glycan-dependent broadly neutralizing antibodies. *Sci Transl Med.*

Table S1. Generation of limiting-dilution isolates from eight epidemiologically linked transmission pairs

Subject	Transmission Partner	Risk Factor	Subtype	Country	Gender	VL	Fiebig Stage*	Number of TF Viruses	Sample	Date	UT	IFNα2 selected	IFNβ selected	Days‡	Accession Codes	
															Isolate Sequences§	SGA Sequences¶
CH0742	Donor	MSM	B	USA	M	112,531			PL	09/10/08	15	3	0		KY112461-KY112478	KY112494-KY112521
						na			SEM	08/27/08	1	0	0		KY112480	
						na			SEM	09/10/08	11	0	0		KY112481-KY112491	
						na			SEM	10/29/08	1	0	0		KY112492	
						na			SEM	12/10/08	1	0	0		KY112493	
						na			SEM	03/18/09	0	0	0			
CH0378	Recipient 1				M	265,936	5	2	PL	08/05/08	17	7	0	36	KY112136-KY112159	KY112160-KY112189
CH0831	Recipient 2				M	261,752	3	1	PL	11/14/08	8	4	4	65#	KY112522-KY112537	KY112538-KY112576
CH0148	Donor	MSM	B	USA	M	246,017			PL	12/19/06	12	3	4		KY112056-KY112074	KY111920-KY111946
CH0040	Recipient				M	298,026	1-2	1†	PL	07/27/06	5	2	0	145	KY112190-KY112196	FJ495827-FJ495838
CH0728	Donor	MTF	B	USA	M	23,965			PL	07/28/08	14	1	0		KY112429-KY112445	KY111983-KY111986 KY112446-KY112460
						na			SEM	07/27/08	0	0	0			
						na			SEM	08/27/08	0	0	0			
						na			SEM	11/04/09	0	0	0			
						na			SEM	05/13/10	0	0	0			
CH0302	Recipient				F	16,218	5	1	PL	04/16/08	7	3	0	103	KY112127-KY112135	KY111947-KY111964, KY364886
CH0492	Donor	FTM	C	MWI	F	472,129			PL	03/11/08	13	19	14		KY112276-KY112321	KY112322-KY112359
						22,753			CVL	02/06/08	17	0	0		KY112259-KY112275	
						7,582			CVL	02/21/08	0	0	0			
						na			CVL	03/11/08	0	0	0			
						14,596			CVL	04/28/08	0	0	0			
CH0427	Recipient				M	1,644,231	1-2	1	PL	01/23/08	10	10	1	47	KY112197-KY112217	KY112218-KY112250
CH0596	Donor	FTM	C	MWI	F	250,981			PL	04/03/08	12	10	6		KY112362-KY112389	KY112390-KY112428
						na			CVL	04/03/08	2	0	0		KY112360-KY112361	
						na			CVL	04/17/08	0	0	0			
CH0455	Recipient				M	502,665	3	1	PL	01/29/08	5	3	0	65	KY112251-KY112258	KY111965-KY111982
CH0212	Donor	FTM	C	ZAF	F	111,427			PL	08/01/07	11	1	0		KY112082-KY112093	KY112094-KY112126
CH0162	Recipient				M	18,260	3	1†	PL	07/13/07	5	2	0	19	KY112075-KY112081	JX972986-JX972998
CH1064	Donor	FTM	C	MWI	F	323,674			PL	04/08/09	18	10	0		KY111987-KY112014	KY112015-KY112055
						bld			CVL	02/11/09	0	0	0			
						bld			CVL	02/25/09	0	0	0			
						na			CVL	04/08/09	0	0	0			
						990			CVL	07/07/09	0	0	0			
CH0848	Recipient				M	361,254	4	1	PL	07/29/08	4	4	0	265	KY112577-KY112584	KX216883-KX216893 KX216895

MSM, men who have sex with men; MTF, male to female; FTM female to male; USA, United States; MWI, Malawi; ZAF, South Africa; M, male; F, female; PL, plasma; SEM, semen; CVL, cervicovaginal lavage; VL, viral load (RNA copies per milliliter of plasma); na, data not available; bld, below limit of detection; UT, untreated. Viral load determination, Fiebig staging, and limiting dilution virus isolation were performed on the same sample from the indicated time point.

*defined as previously described (2).

†infectious molecular clone (IMC) available

‡number of days between recipient and first available donor samples.

#in contrast to all other recipients, CH831 was sampled 64 days after donor CH742.

§Isolate sequences represent near-complete viral genomes (8,750-9,208 bp).

¶SGA sequences span *rev-vpu-env-nef* gene regions (2,922-2,973 bp for KY112446-KY112460) or 3' half genomes (4,112-4,936 bp).

Table S2A. Genealogical sorting index analysis of sequences from uncultured plasma and limiting dilution isolates

Donor	Plasma SGA	Plasma Isolates
CH1064	0.039	0.120
CH148	0.059	0.092
CH212	0.142	0.421**
CH492	0.119	0.100
CH596	0.065	0.110
CH728[§]	0.346*	0.136
CH742	0.090	0.224

To assess to what extent viral isolates were representative of the virus present in the plasma of the chronically infected donors, we constructed maximum likelihood phylogenetic trees from 3' half genome or *env* gene[§] sequences and used these to assess the degree of segregation between single genome amplification derived plasma (Plasma SGA) and limiting dilution derived isolate (Plasma Isolates) sequences by determining their genealogical sorting index (gsi) (21). Gsi indices range between 0 (no segregation) and 1 (complete monophyly) and were calculated using the genealogical Sorting R package (http://molecularevolution.org/software/phylogenetics/gsi/download). Two gsi values, which were significantly higher than expected from random segregation, are indicated (* $p<0.05$; ** $p < 0.01$). For CH212, available plasma isolates represented only two of three diverse viral lineages present in this donor's quasispecies, indicating insufficient sampling (Fig. S3*F*). For CH728, the high gsi value was due to two clusters of near identical isolate sequences, indicating repeat culture of the same virus (Fig. S3*C*). Collapsing one of these clusters to a single sequence reduced the Plasma SGA and Plasma Isolate gsi values to non-significant values (0.3 and 0.116, respectively). For all other donors, limiting dilution isolates were fully representative of the viral diversity present in the plasma. Statistical significance was assessed by randomly permuting character states across the tips of the tree 10,000 times (p values were corrected for multiple tests).

Table S2B. Genealogical sorting index analysis of sequences from plasma and genital secretion isolates

Donor	Genital Secretion Isolates	Plasma Isolates
CH492	0.142	0.225
CH742	0.236	0.333*

To assess the extent of segregation of plasma and CVL isolates for donor CH492, and plasma and semen isolates for donor CH742, we constructed maximum likelihood trees of full-length plasma and genital secretion isolate sequences, and used these to calculate the genealogical sorting index (http://molecularevolution.org/software/phylogenetics/gsi/download) (21). Gsi indices range between 0 (no segregation) and 1 (complete monophyly), and values that were significantly higher than expected from random segregation are indicated (* $p<0.05$). For CH742, the high gsi value was due to a pair of nearly identical semen isolate sequences, indicating repeat culture of the same virus (Fig. S3*A*). Collapsing this cluster to a single sequence reduced the genital secretion and plasma isolates gsi values to non-significant values (0.229 and 0.187, respectively). Statistical significance was assessed by randomly permuting character states across the tips of the tree 10,000 times. Non-significant values indicate the absence of compartmentalization (p values were corrected for multiple tests).

Table S2C. Genealogical sorting index analysis of sequences from IFN-selected and untreated plasma isolates

Donor	IFN-Selected	Untreated
CH1064	0.175	0
CH148	0.143	0
CH492	0.136	0.112
CH596	0.124	0.094
CH742	0.095	0

To assess the extent of segregation of plasma isolates generated in IFN-selected and untreated CD4+ T cells, we constructed maximum likelihood trees of full-length isolate sequences and calculated their genealogical sorting index (gsi) (21) using the genealogical Sorting R package (http://molecularevolution.org/software/phylogenetics/gsi/download). Gsi indices range between 0 (no segregation) and 1 (complete monophyly). Statistical significance was assessed by randomly permuting character states across the tips of the tree 10,000 times. None of the values was significant, indicating complete interspersion (p values were corrected for multiple tests).

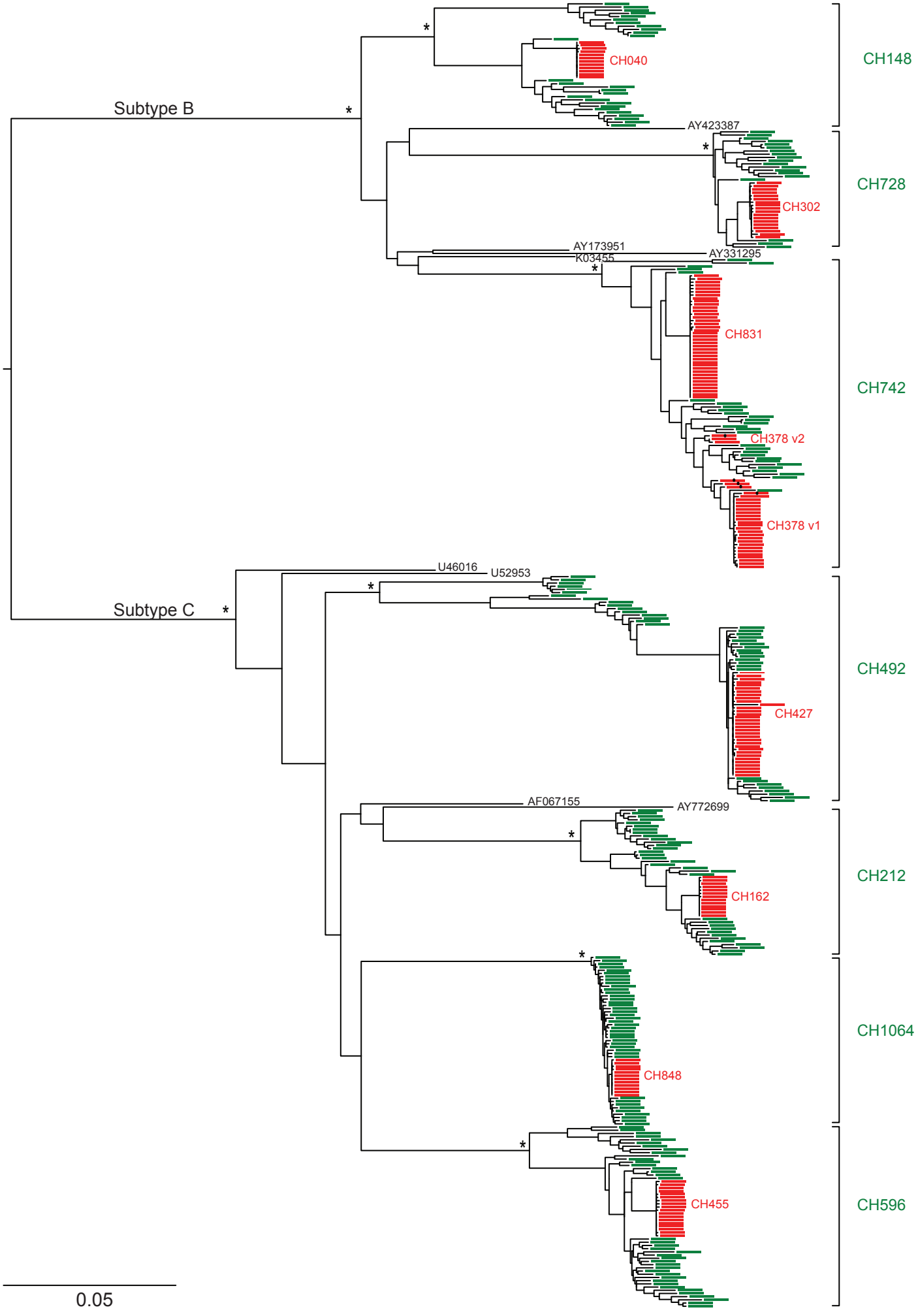
Subtype B
Subtype C
CH040
AY423387
CH302
AY173951
K03455
AY331295
CH831
CH378 v2
CH378 v1
U46016
U52953
CH427
AF067155
AY772699
CH162
CH848
CH455
CH148
CH728
CH742
CH492
CH212
CH1064
CH596
0.05

Fig. S1. Confirmation of epidemiological linkage of transmission pairs. 3' half genome sequences were generated by single genome amplification (SGA) of viral RNA from the plasma of respective donors and recipients. Nucleotide sequences of partial *tat*, partial *rev*, *vpu*, *env* and partial *nef* genes were aligned using CLUSTALW v. 2 (16), with ambiguous regions removed (the 2,654 bp alignment spans HXB2 coordinates 5,984-8,866). A maximum likelihood tree with bootstrap support (1,000 replicates) was constructed using RAxML v. 8.0.22 (20) with a GTRGAMMA evolutionary model. Sequences from donors and acutely infected recipients are indicated by green and red rectangles, respectively, with brackets denoting individual transmission pairs. Donor CH742 transmitted to two recipients (Fig. S2), one of whom (CH378) acquired two transmitted founder viruses (v1 and v2). Also shown for CH378 are sequences that are recombinant between v1 and v2 (red rectangles with black circles). Subtype B reference sequences (labeled by accession code) included HXB2 (K03455), BK132 (AY173951), 1058 (AY331295) and 671_00T36 (AY423387), while subtype C reference sequences included ETH2220 (U46016), BR025 (U52935), 95IN21068 (AF067155) and 04ZASK146 (AY772699). Asterisks indicate nodes with ≥ 95% bootstrap support (the scale bar represents 0.05 substitutions per site).

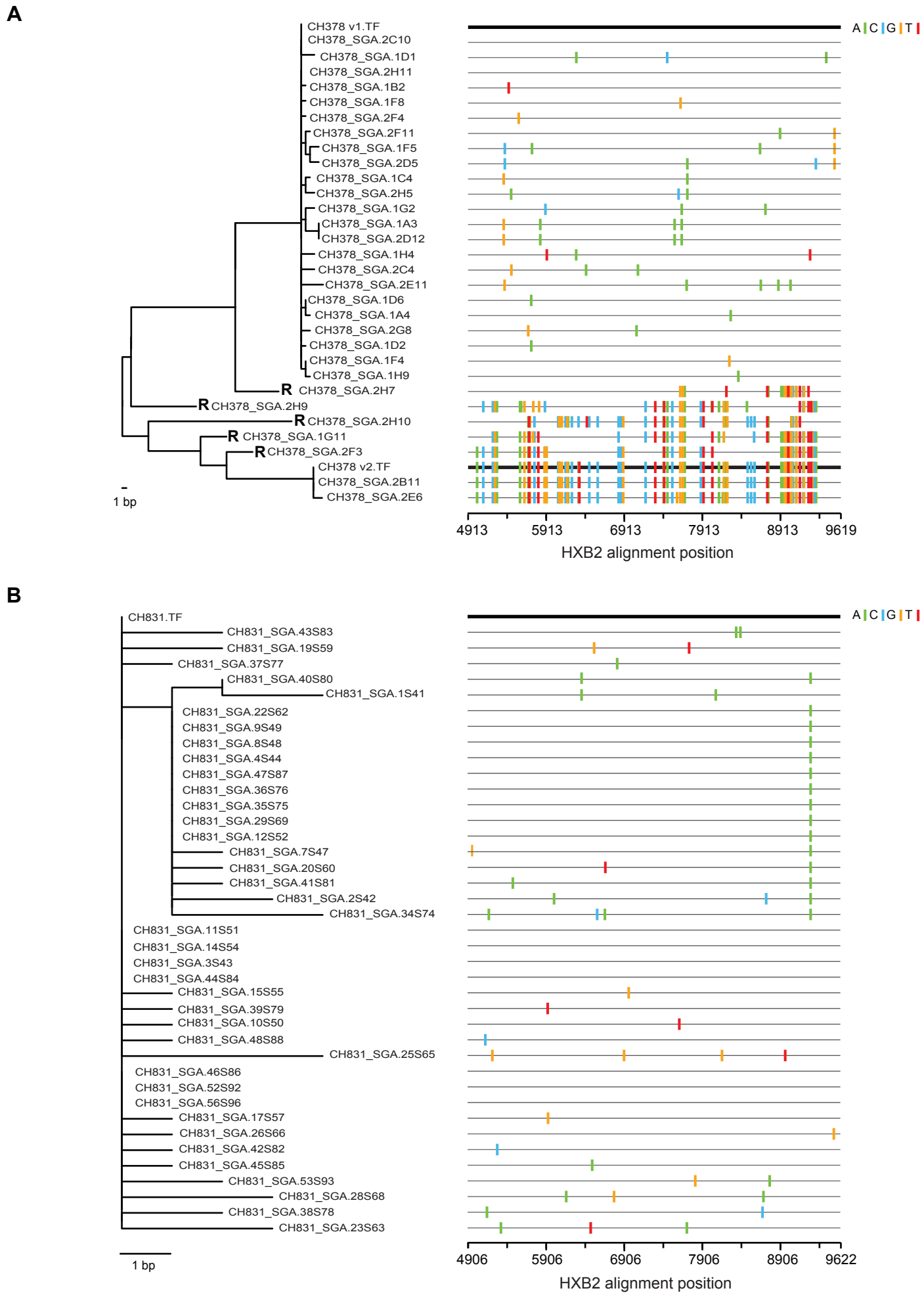
A
CH378 v1.TF
CH378_SGA.2C10
CH378_SGA.1D1
CH378_SGA.2H11
CH378_SGA.1B2
CH378_SGA.1F8
CH378_SGA.2F4
CH378_SGA.2F11
CH378_SGA.1F5
CH378_SGA.2D5
CH378_SGA.1C4
CH378_SGA.2H5
CH378_SGA.1G2
CH378_SGA.1A3
CH378_SGA.2D12
CH378_SGA.1H4
CH378_SGA.2C4
CH378_SGA.2E11
CH378_SGA.1D6
CH378_SGA.1A4
CH378_SGA.2G8
CH378_SGA.1D2
CH378_SGA.1F4
CH378_SGA.1H9
R CH378_SGA.2H7
R CH378_SGA.2H9
R CH378_SGA.2H10
R CH378_SGA.1G11
R CH378_SGA.2F3
CH378 v2.TF
CH378_SGA.2B11
CH378_SGA.2E6
1 bp
A C G T
4913
5913
6913
7913
8913
9619
HXB2 alignment position
B
CH831.TF
CH831_SGA.43S83
CH831_SGA.19S59
CH831_SGA.37S77
CH831_SGA.40S80
CH831_SGA.1S41
CH831_SGA.22S62
CH831_SGA.9S49
CH831_SGA.8S48
CH831_SGA.4S44
CH831_SGA.47S87
CH831_SGA.36S76
CH831_SGA.35S75
CH831_SGA.29S69
CH831_SGA.12S52
CH831_SGA.7S47
CH831_SGA.20S60
CH831_SGA.41S81
CH831_SGA.2S42
CH831_SGA.34S74
CH831_SGA.11S51
CH831_SGA.14S54
CH831_SGA.3S43
CH831_SGA.44S84
CH831_SGA.15S55
CH831_SGA.39S79
CH831_SGA.10S50
CH831_SGA.48S88
CH831_SGA.25S65
CH831_SGA.46S86
CH831_SGA.52S92
CH831_SGA.56S96
CH831_SGA.17S57
CH831_SGA.26S66
CH831_SGA.42S82
CH831_SGA.45S85
CH831_SGA.53S93
CH831_SGA.28S68
CH831_SGA.38S78
CH831_SGA.23S63
1 bp
A C G T
4906
5906
6906
7906
8906
9622
HXB2 alignment position

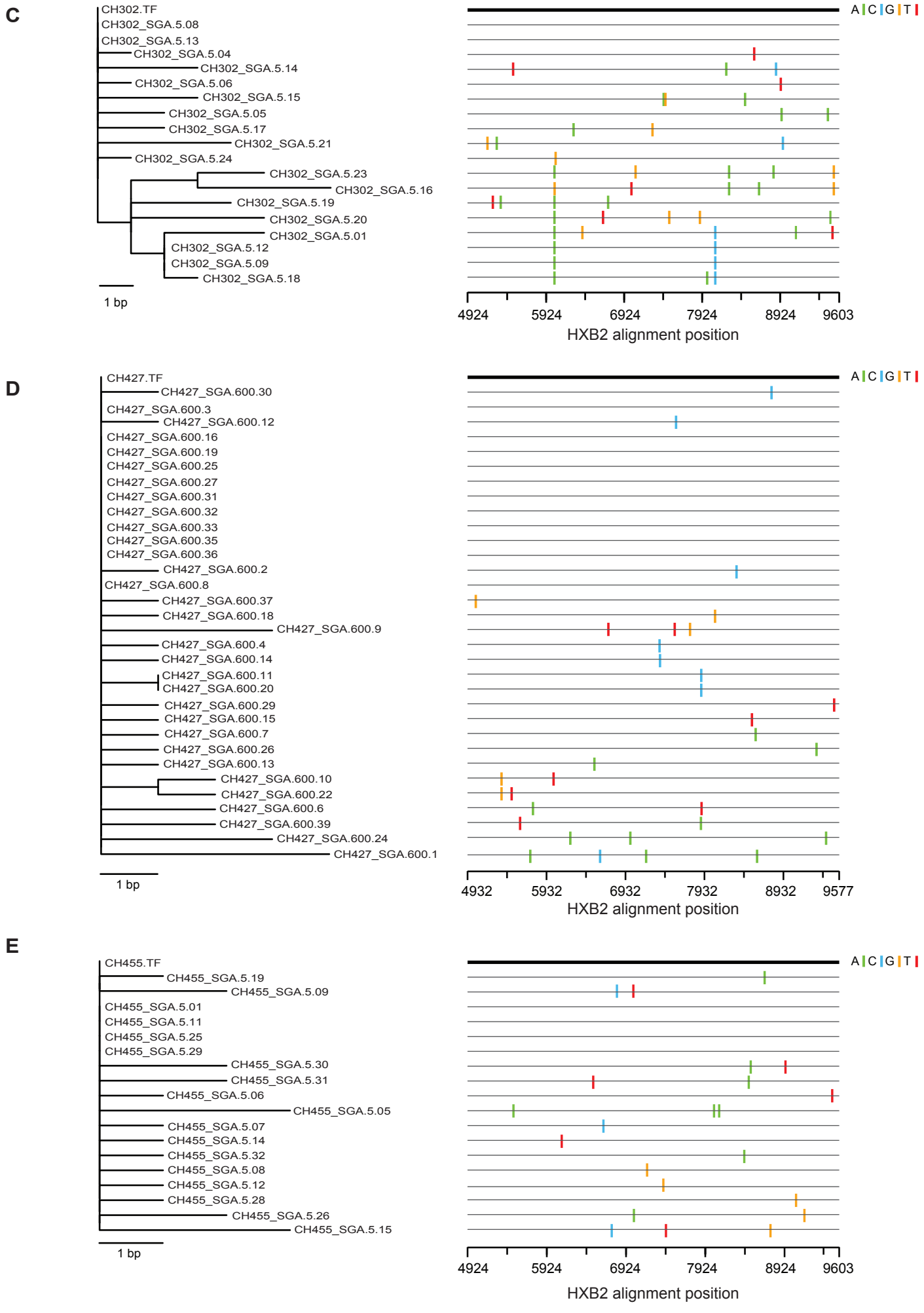
C
CH302.TF
CH302_SGA.5.08
CH302_SGA.5.13
CH302_SGA.5.04
CH302_SGA.5.14
CH302_SGA.5.06
CH302_SGA.5.15
CH302_SGA.5.05
CH302_SGA.5.17
CH302_SGA.5.21
CH302_SGA.5.24
CH302_SGA.5.23
CH302_SGA.5.16
CH302_SGA.5.19
CH302_SGA.5.20
CH302_SGA.5.01
CH302_SGA.5.12
CH302_SGA.5.09
CH302_SGA.5.18
1 bp
A C G T
4924
5924
6924
7924
8924
9603
HXB2 alignment position
D
CH427.TF
CH427_SGA.600.30
CH427_SGA.600.3
CH427_SGA.600.12
CH427_SGA.600.16
CH427_SGA.600.19
CH427_SGA.600.25
CH427_SGA.600.27
CH427_SGA.600.31
CH427_SGA.600.32
CH427_SGA.600.33
CH427_SGA.600.35
CH427_SGA.600.36
CH427_SGA.600.2
CH427_SGA.600.8
CH427_SGA.600.37
CH427_SGA.600.18
CH427_SGA.600.9
CH427_SGA.600.4
CH427_SGA.600.14
CH427_SGA.600.11
CH427_SGA.600.20
CH427_SGA.600.29
CH427_SGA.600.15
CH427_SGA.600.7
CH427_SGA.600.26
CH427_SGA.600.13
CH427_SGA.600.10
CH427_SGA.600.22
CH427_SGA.600.6
CH427_SGA.600.39
CH427_SGA.600.24
CH427_SGA.600.1
1 bp
A C G T
4932
5932
6932
7932
8932
9577
HXB2 alignment position
E
CH455.TF
CH455_SGA.5.19
CH455_SGA.5.09
CH455_SGA.5.01
CH455_SGA.5.11
CH455_SGA.5.25
CH455_SGA.5.29
CH455_SGA.5.30
CH455_SGA.5.31
CH455_SGA.5.06
CH455_SGA.5.05
CH455_SGA.5.07
CH455_SGA.5.14
CH455_SGA.5.32
CH455_SGA.5.08
CH455_SGA.5.12
CH455_SGA.5.28
CH455_SGA.5.26
CH455_SGA.5.15
1 bp
A C G T
4924
5924
6924
7924
8924
9603
HXB2 alignment position

Fig. S2. **Transmitted founder sequence inference and enumeration.** Neighbor-joining phylogenetic trees (left) and highlighter plots (right) were generated for SGA derived 3' half genome sequences using the Los Alamos National Laboratory HIV Sequence Database Highlighter Tool (5). In the phylogenetic trees, the inferred transmitted founder (TF) sequence is shown at the top. The scale bar represents one base pair difference. In the highlighter plots, the TF sequence is used as the reference and indicated by a thick line. Thinner lines below correspond to sequences shown in the phylogenetic tree to the left. Tick marks indicate nucleotide differences from the TF sequence (green, A; blue, C; G orange; T, red). (*A*) Sequences from the acute recipient CH378 (4,774 bp) span HXB2 coordinates 4,913-9,619. For this recipient, two TF variants (v1 and v2) were identified. The former was used as a reference for the highlighter plot, but both variants are shown as thick lines. A bold-faced R preceding the sequence name indicates recombinants between these two variants. (*B*) Sequences from recipient CH831 (4,783 bp) span HXB2 coordinates 4906-9622. (*C*) Sequences from recipient CH302 (4,757 bp) span HXB2 coordinates 4924-9603. (*D*) Sequences from recipient CH427 (4,674 bp) span HXB2 coordinates 4932-9577. (*E*) Sequences from recipient CH455 (4,696 bp) span HXB2 coordinates 4924-9603. TF sequence inference and enumeration of the remaining three recipients (CH040, CH162, and CH848) have been published (4, 12, 27).

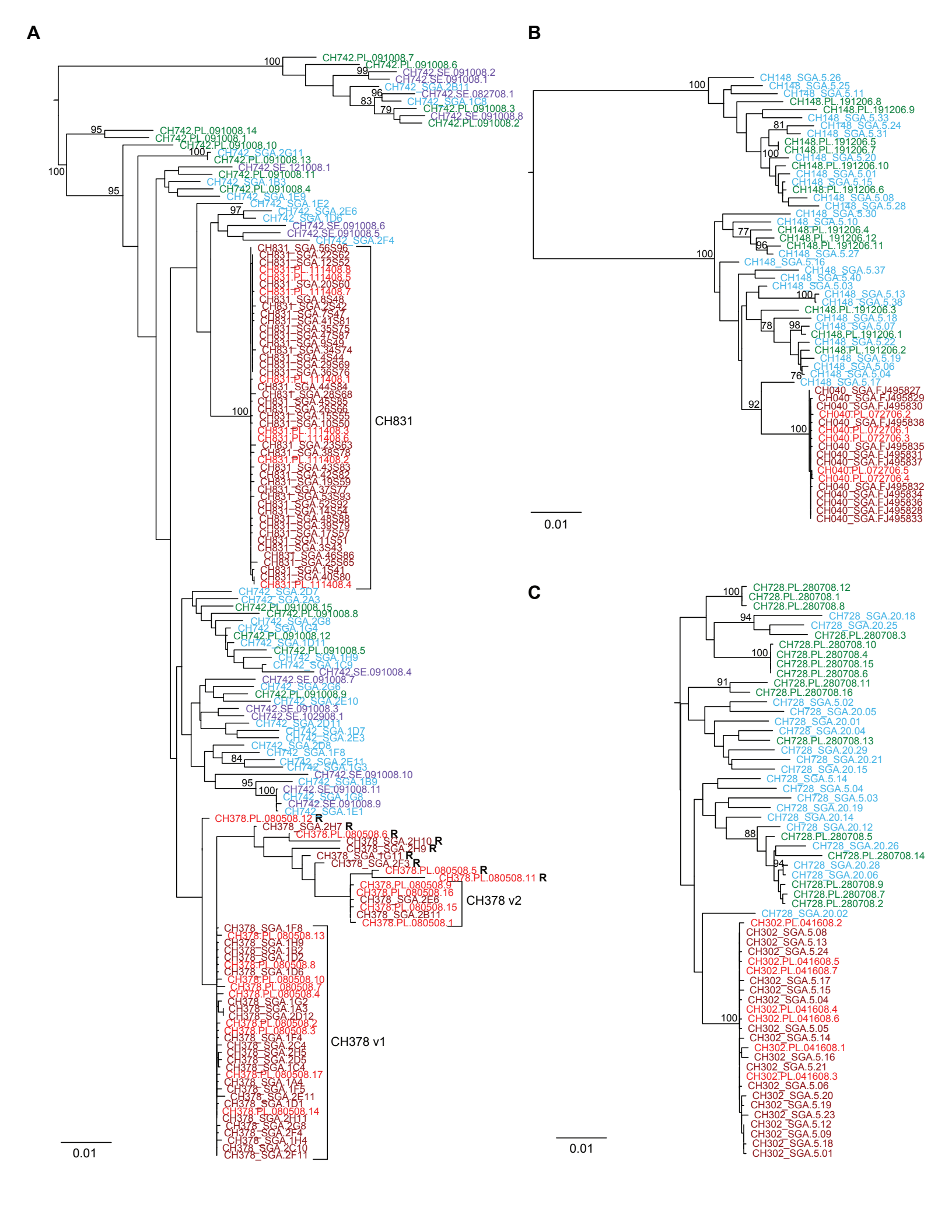
A
B
C
CH831
CH378 v2
CH378 v1
0.01
0.01
0.01

D

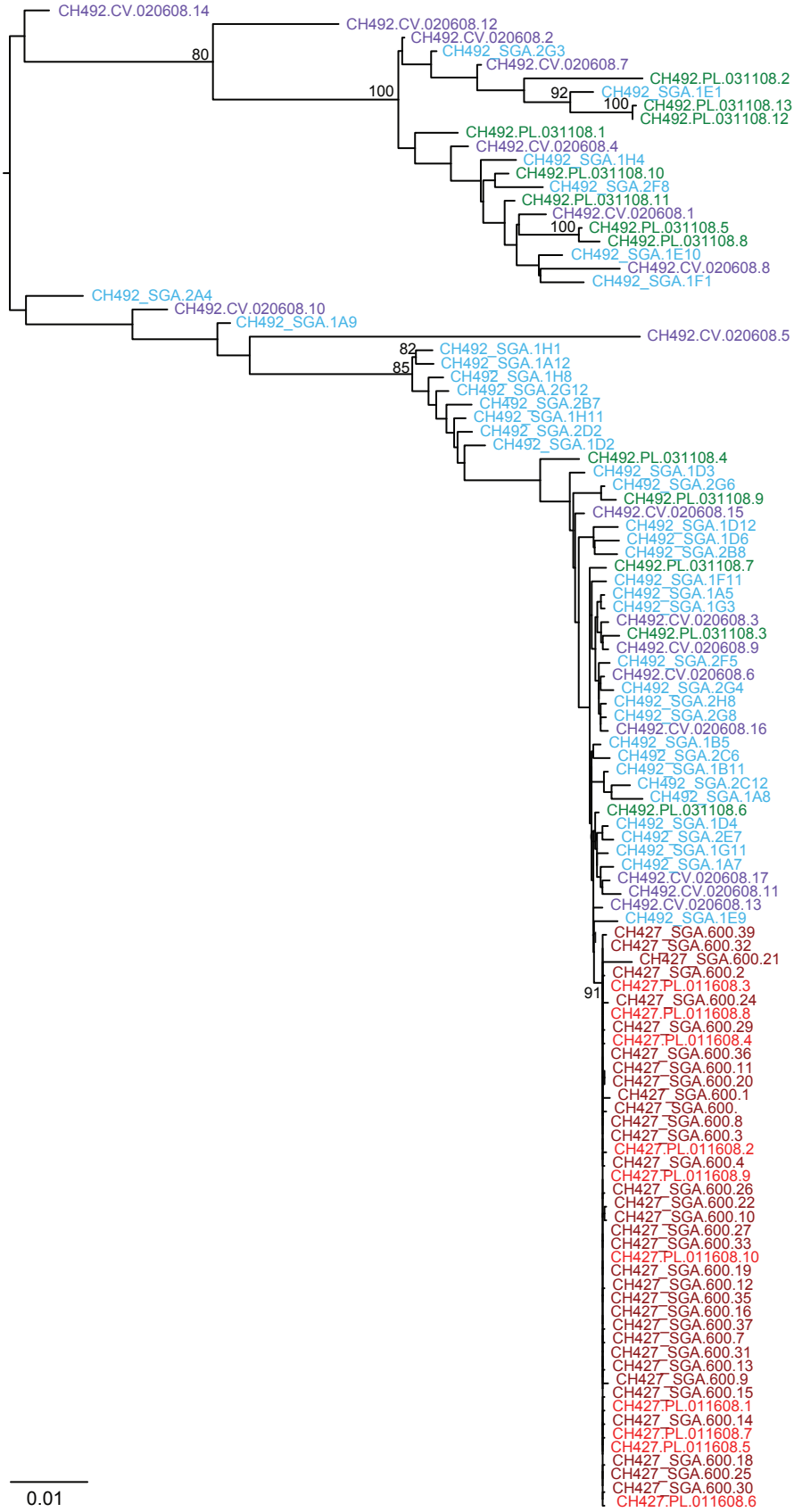
CH492.CV.020608.14
CH492.CV.020608.12
CH492.CV.020608.2
CH492_SGA.2G3
CH492.CV.020608.7
CH492.PL.031108.2
CH492_SGA.1E1
CH492.PL.031108.13
CH492.PL.031108.12
CH492.PL.031108.1
CH492.CV.020608.4
CH492_SGA.1H4
CH492.PL.031108.10
CH492_SGA.2F8
CH492.PL.031108.11
CH492.CV.020608.1
CH492.PL.031108.5
CH492.PL.031108.8
CH492_SGA.1E10
CH492.CV.020608.8
CH492_SGA.1F1
CH492_SGA.2A4
CH492.CV.020608.10
CH492_SGA.1A9
CH492.CV.020608.5
CH492_SGA.1H1
CH492_SGA.1A12
CH492_SGA.1H8
CH492_SGA.2G12
CH492_SGA.2B7
CH492_SGA.1H11
CH492_SGA.2D2
CH492_SGA.1D2
CH492.PL.031108.4
CH492_SGA.1D3
CH492_SGA.2G6
CH492.PL.031108.9
CH492.CV.020608.15
CH492_SGA.1D12
CH492_SGA.1D6
CH492_SGA.2B8
CH492.PL.031108.7
CH492_SGA.1F11
CH492_SGA.1A5
CH492_SGA.1G3
CH492.CV.020608.3
CH492.PL.031108.3
CH492.CV.020608.9
CH492_SGA.2F5
CH492.CV.020608.6
CH492_SGA.2G4
CH492_SGA.2H8
CH492_SGA.2G8
CH492.CV.020608.16
CH492_SGA.1B5
CH492_SGA.2C6
CH492_SGA.1B11
CH492_SGA.2C12
CH492_SGA.1A8
CH492.PL.031108.6
CH492_SGA.1D4
CH492_SGA.2E7
CH492_SGA.1G11
CH492_SGA.1A7
CH492.CV.020608.17
CH492.CV.020608.11
CH492.CV.020608.13
CH492_SGA.1E9
CH427_SGA.600.39
CH427_SGA.600.32
CH427_SGA.600.21
CH427_SGA.600.2
CH427.PL.011608.3
CH427_SGA.600.24
CH427.PL.011608.8
CH427_SGA.600.29
CH427.PL.011608.4
CH427_SGA.600.36
CH427_SGA.600.11
CH427_SGA.600.20
CH427_SGA.600.1
CH427_SGA.600.
CH427_SGA.600.8
CH427_SGA.600.3
CH427.PL.011608.2
CH427_SGA.600.4
CH427.PL.011608.9
CH427_SGA.600.26
CH427_SGA.600.22
CH427_SGA.600.10
CH427_SGA.600.27
CH427_SGA.600.33
CH427.PL.011608.10
CH427_SGA.600.19
CH427_SGA.600.12
CH427_SGA.600.35
CH427_SGA.600.16
CH427_SGA.600.37
CH427_SGA.600.7
CH427_SGA.600.31
CH427_SGA.600.13
CH427_SGA.600.9
CH427_SGA.600.15
CH427.PL.011608.1
CH427_SGA.600.14
CH427.PL.011608.7
CH427.PL.011608.5
CH427_SGA.600.18
CH427_SGA.600.25
CH427_SGA.600.30
CH427.PL.011608.6
80
100
92
100
100
82
85
91
0.01

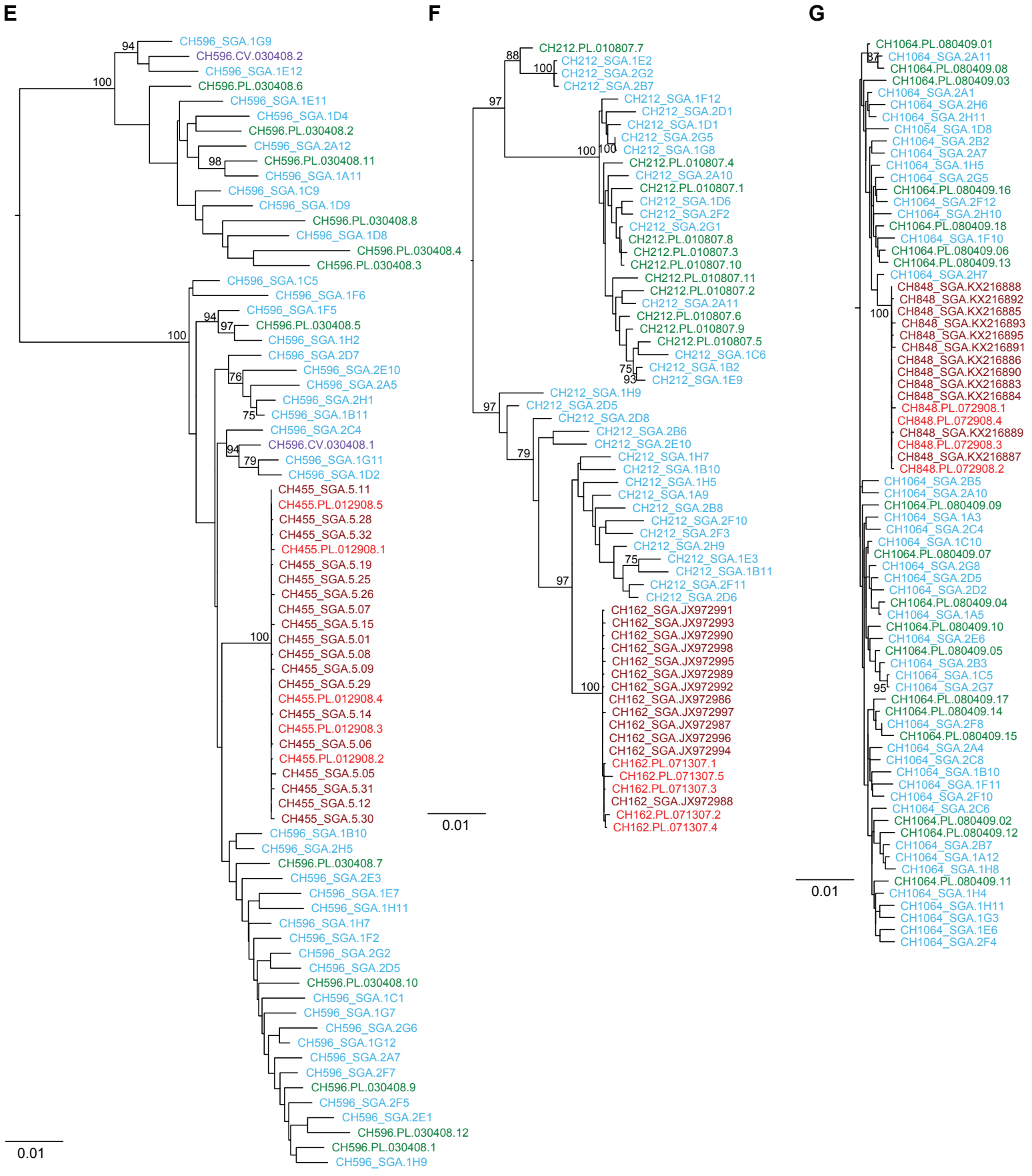
E
CH596_SGA.1G9
CH596.CV.030408.2
CH596_SGA.1E12
CH596.PL.030408.6
CH596_SGA.1E11
CH596_SGA.1D4
CH596.PL.030408.2
CH596_SGA.2A12
CH596.PL.030408.11
CH596_SGA.1A11
CH596_SGA.1C9
CH596_SGA.1D9
CH596.PL.030408.8
CH596_SGA.1D8
CH596.PL.030408.4
CH596.PL.030408.3
CH596_SGA.1C5
CH596_SGA.1F6
CH596_SGA.1F5
CH596.PL.030408.5
CH596_SGA.1H2
CH596_SGA.2D7
CH596_SGA.2E10
CH596_SGA.2A5
CH596_SGA.2H1
CH596_SGA.1B11
CH596_SGA.2C4
CH596.CV.030408.1
CH596_SGA.1G11
CH596_SGA.1D2
CH455_SGA.5.11
CH455.PL.012908.5
CH455_SGA.5.28
CH455_SGA.5.32
CH455.PL.012908.1
CH455_SGA.5.19
CH455_SGA.5.25
CH455_SGA.5.26
CH455_SGA.5.07
CH455_SGA.5.15
CH455_SGA.5.01
CH455_SGA.5.08
CH455_SGA.5.09
CH455_SGA.5.29
CH455.PL.012908.4
CH455_SGA.5.14
CH455.PL.012908.3
CH455_SGA.5.06
CH455.PL.012908.2
CH455_SGA.5.05
CH455_SGA.5.31
CH455_SGA.5.12
CH455_SGA.5.30
CH596_SGA.1B10
CH596_SGA.2H5
CH596.PL.030408.7
CH596_SGA.2E3
CH596_SGA.1E7
CH596_SGA.1H11
CH596_SGA.1H7
CH596_SGA.1F2
CH596_SGA.2G2
CH596_SGA.2D5
CH596.PL.030408.10
CH596_SGA.1C1
CH596_SGA.1G7
CH596_SGA.2G6
CH596_SGA.1G12
CH596_SGA.2A7
CH596_SGA.2F7
CH596.PL.030408.9
CH596_SGA.2F5
CH596_SGA.2E1
CH596.PL.030408.12
CH596.PL.030408.1
CH596_SGA.1H9
0.01
F
CH212.PL.010807.7
CH212_SGA.1E2
CH212_SGA.2G2
CH212_SGA.2B7
CH212_SGA.1F12
CH212_SGA.2D1
CH212_SGA.1D1
CH212_SGA.2G5
CH212_SGA.1G8
CH212.PL.010807.4
CH212_SGA.2A10
CH212.PL.010807.1
CH212_SGA.1D6
CH212_SGA.2F2
CH212_SGA.2G1
CH212.PL.010807.8
CH212.PL.010807.3
CH212.PL.010807.10
CH212.PL.010807.11
CH212.PL.010807.2
CH212_SGA.2A11
CH212.PL.010807.6
CH212.PL.010807.9
CH212.PL.010807.5
CH212_SGA.1C6
CH212_SGA.1B2
CH212_SGA.1E9
CH212_SGA.1H9
CH212_SGA.2D5
CH212_SGA.2D8
CH212_SGA.2B6
CH212_SGA.2E10
CH212_SGA.1H7
CH212_SGA.1B10
CH212_SGA.1H5
CH212_SGA.1A9
CH212_SGA.2B8
CH212_SGA.2F10
CH212_SGA.2F3
CH212_SGA.2H9
CH212_SGA.1E3
CH212_SGA.1B11
CH212_SGA.2F11
CH212_SGA.2D6
CH162_SGA.JX972991
CH162_SGA.JX972993
CH162_SGA.JX972990
CH162_SGA.JX972998
CH162_SGA.JX972995
CH162_SGA.JX972989
CH162_SGA.JX972992
CH162_SGA.JX972986
CH162_SGA.JX972997
CH162_SGA.JX972987
CH162_SGA.JX972996
CH162_SGA.JX972994
CH162.PL.071307.1
CH162.PL.071307.5
CH162.PL.071307.3
CH162_SGA.JX972988
CH162.PL.071307.2
CH162.PL.071307.4
0.01
G
CH1064.PL.080409.01
CH1064_SGA.2A11
CH1064.PL.080409.08
CH1064.PL.080409.03
CH1064_SGA.2A1
CH1064_SGA.2H6
CH1064_SGA.2H11
CH1064_SGA.1D8
CH1064_SGA.2B2
CH1064_SGA.2A7
CH1064_SGA.1H5
CH1064_SGA.2G5
CH1064.PL.080409.16
CH1064_SGA.2F12
CH1064_SGA.2H10
CH1064.PL.080409.18
CH1064_SGA.1F10
CH1064.PL.080409.06
CH1064.PL.080409.13
CH1064_SGA.2H7
CH848_SGA.KX216888
CH848_SGA.KX216892
CH848_SGA.KX216885
CH848_SGA.KX216893
CH848_SGA.KX216895
CH848_SGA.KX216891
CH848_SGA.KX216886
CH848_SGA.KX216890
CH848_SGA.KX216883
CH848_SGA.KX216884
CH848.PL.072908.1
CH848.PL.072908.4
CH848_SGA.KX216889
CH848.PL.072908.3
CH848_SGA.KX216887
CH848.PL.072908.2
CH1064_SGA.2B5
CH1064_SGA.2A10
CH1064.PL.080409.09
CH1064_SGA.1A3
CH1064_SGA.2C4
CH1064_SGA.1C10
CH1064.PL.080409.07
CH1064_SGA.2G8
CH1064_SGA.2D5
CH1064_SGA.2D2
CH1064.PL.080409.04
CH1064_SGA.1A5
CH1064.PL.080409.10
CH1064_SGA.2E6
CH1064.PL.080409.05
CH1064_SGA.2B3
CH1064_SGA.1C5
CH1064_SGA.2G7
CH1064.PL.080409.17
CH1064.PL.080409.14
CH1064_SGA.2F8
CH1064.PL.080409.15
CH1064_SGA.2A4
CH1064_SGA.2C8
CH1064_SGA.1B10
CH1064_SGA.1F11
CH1064_SGA.2F10
CH1064_SGA.2C6
CH1064.PL.080409.02
CH1064.PL.080409.12
CH1064_SGA.2B7
CH1064_SGA.1A12
CH1064_SGA.1H8
CH1064.PL.080409.11
CH1064_SGA.1H4
CH1064_SGA.1H11
CH1064_SGA.1G3
CH1064_SGA.1E6
CH1064_SGA.2F4
0.01

Fig. S3. Limiting dilution-derived isolates are representative of the viral quasispecies present *in vivo*. The phylogenetic relationships of limiting dilution-derived isolate and SGA-derived plasma viral sequences are shown for all transmission pairs. Maximum likelihood trees with bootstrap support (1,000 replicates) were constructed using PhyML v. 3.1 (17) with evolutionary models selected using jModelTest v. 2.1.4 (19). For transmitting donors, plasma isolates (labeled PL, followed by the date and the isolate number), genital secretion isolates (labeled SE for semen and CV for cervicovaginal lavage, followed by the date and isolate number), and plasma vRNA derived SGA sequences (labeled SGA, followed by the amplicon number) are indicated in green, purple and blue, respectively. For acutely infected recipients, plasma isolate and SGA sequences (labeled like donor isolates) are shown in red and brown, respectively. Nodes with ≥ 75% bootstrap support are indicated (the scale bars represent 0.01 substitutions per site). (*A*) 3' half genome sequences from donor CH742 and his two recipients CH831 and CH378 denoted by brackets (4,358 bp). CH378 acquired two TF viruses, termed v1 and v2 (recombinants of these are labeled R). (*B*) 3' half genome sequences from donor CH148 and recipient CH040 (4,481 bp). SGA sequences for CH040 are available under GenBank accession codes: FJ495827 - FJ495838. (*C*) *tat*/*rev*, *env* and *nef* sequences from donor CH728 and recipient CH302 (2,829 bp). (*D*) 3' half genome sequences from donor CH492 and recipient CH427 (4,539 bp). (*E*) 3' half genome sequences from donor CH596 and recipient CH455 (4,501 bp). (*F*) 3' half genome sequences from donor CH212 and recipient CH162 (4,463 bp). SGA sequences for CH162 are available under GenBank accession codes: JX972986 - JX972998. (*G*) 3' half genome sequences from donor CH1064 and recipient CH848 (4,550 bp). SGA sequences for CH848 are available under GenBank accession codes: KX216883 - KX216893 and KX216895.

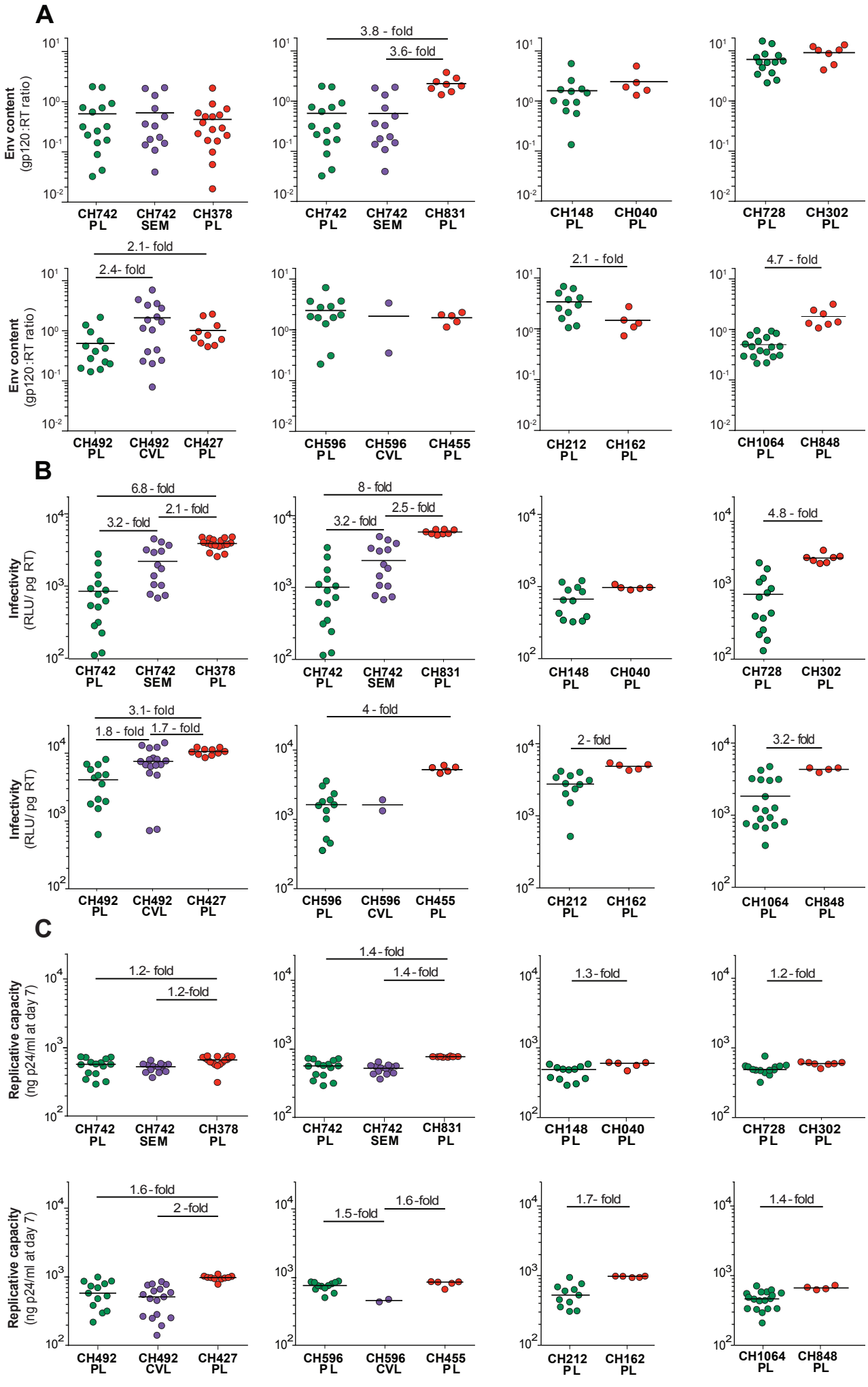
A
Env content (gp120:RT ratio)
CH742 PL
CH742 SEM
CH378 PL
3.8 - fold
3.6- fold
CH831 PL
CH148 PL
CH040 PL
CH728 PL
CH302 PL
2.1- fold
2.4- fold
CH492 PL
CH492 CVL
CH427 PL
CH596 PL
CH596 CVL
CH455 PL
2.1 - fold
CH212 PL
CH162 PL
4.7 - fold
CH1064 PL
CH848 PL
B
Infectivity (RLU/ pg RT)
6.8 - fold
2.1 - fold
3.2 - fold
8 - fold
2.5 - fold
4.8 - fold
3.1- fold
1.8 - fold
1.7 - fold
4 - fold
2 - fold
3.2- fold
C
Replicative capacity (ng p24/ml at day 7)
1.2- fold
1.2-fold
1.4 - fold
1.3 - fold
1.6 - fold
2 -fold
1.5 - fold
1.7- fold
1.4 - fold

Fig. S4. Env content, particle infectivity and replicative capacity of limiting dilution-derived isolates from matched donor and recipient pairs. (*A*) Env content (gp120:RT mass ratio), (*B*) particle infectivity (relative light units [RLU] in the TZM-bl assay per picogram of RT), and (*C*) replicative capacity (ng of p24 per ml of CD4 T cell culture supernatant at day 7 post infection) are shown for each limiting dilution-derived isolate of each transmission pair. Each dot represents an individual isolate derived from donor plasma (PL, green), donor genital secretions (CVL or SEM, purple), or recipient plasma (PL, red). Black lines denote the geometric mean, and fold changes are listed above groups when significant ($P < 0.05$).

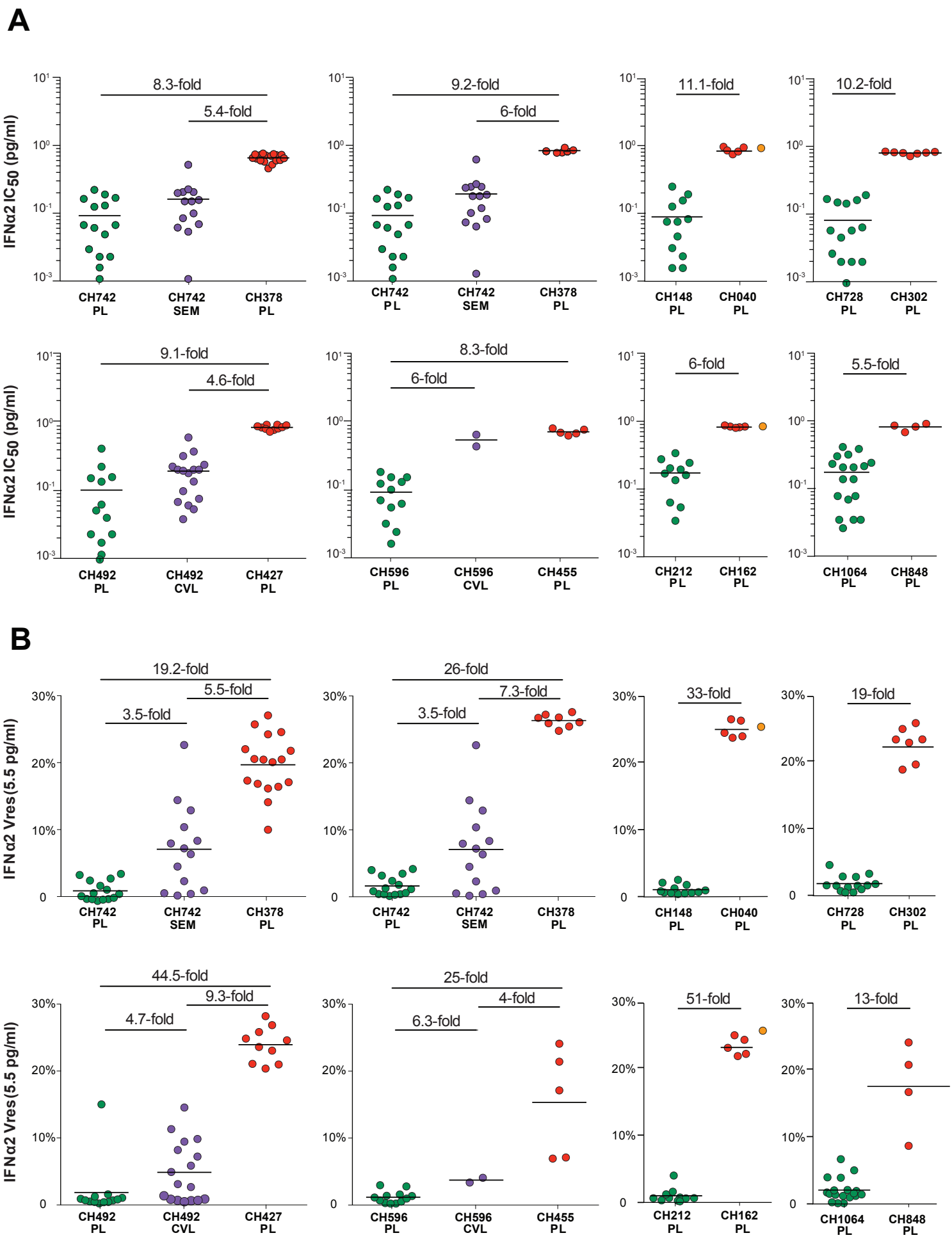
A
IFNα2 IC50 (pg/ml)
8.3-fold
5.4-fold
CH742 PL
CH742 SEM
CH378 PL
9.2-fold
6-fold
CH742 PL
CH742 SEM
CH378 PL
11.1-fold
CH148 PL
CH040 PL
10.2-fold
CH728 PL
CH302 PL
9.1-fold
4.6-fold
CH492 PL
CH492 CVL
CH427 PL
8.3-fold
6-fold
CH596 PL
CH596 CVL
CH455 PL
6-fold
CH212 PL
CH162 PL
5.5-fold
CH1064 PL
CH848 PL
B
IFNα2 Vres(5.5 pg/ml)
19.2-fold
5.5-fold
3.5-fold
CH742 PL
CH742 SEM
CH378 PL
26-fold
7.3-fold
3.5-fold
CH742 PL
CH742 SEM
CH378 PL
33-fold
CH148 PL
CH040 PL
19-fold
CH728 PL
CH302 PL
44.5-fold
9.3-fold
4.7-fold
CH492 PL
CH492 CVL
CH427 PL
25-fold
4-fold
6.3-fold
CH596 PL
CH596 CVL
CH455 PL
51-fold
CH212 PL
CH162 PL
13-fold
CH1064 PL
CH848 PL

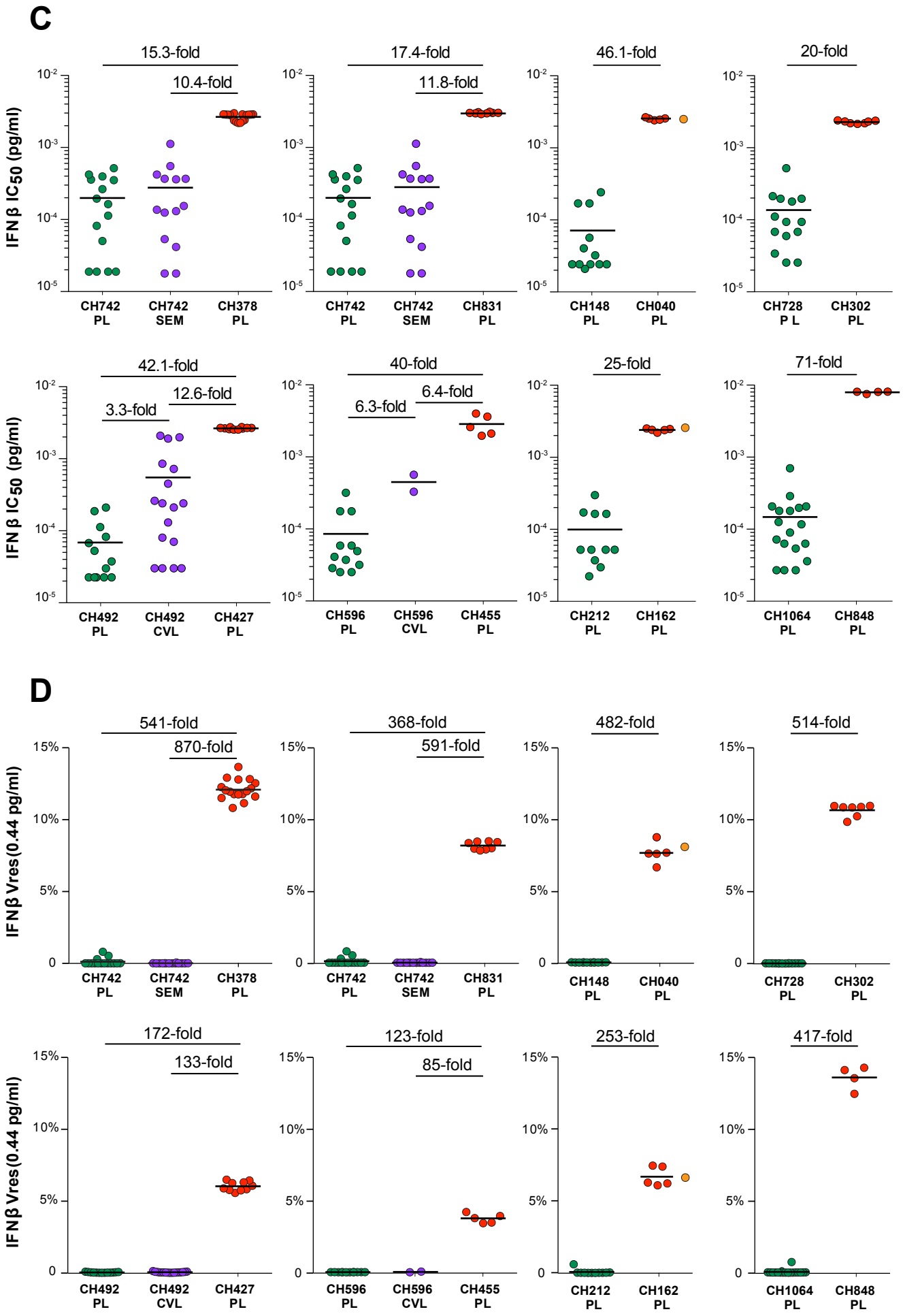
C
IFN β IC50 (pg/ml)
15.3-fold
10.4-fold
17.4-fold
11.8-fold
46.1-fold
20-fold
42.1-fold
3.3-fold
12.6-fold
40-fold
6.3-fold
6.4-fold
25-fold
71-fold
CH742 PL
CH742 SEM
CH378 PL
CH831 PL
CH148 PL
CH040 PL
CH728 P L
CH302 PL
CH492 PL
CH492 CVL
CH427 PL
CH596 PL
CH596 CVL
CH455 PL
CH212 PL
CH162 PL
CH1064 PL
CH848 PL
D
IFN β Vres(0.44 pg/ml)
541-fold
870-fold
368-fold
591-fold
482-fold
514-fold
172-fold
133-fold
123-fold
85-fold
253-fold
417-fold

Fig. S5. IFN resistance of limiting dilution-derived isolates from matched donor and recipient pairs. Donor and recipient isolates were tested for their sensitivity to inhibition by type 1 IFNs. (*A*) Half-maximal inhibitory concentrations (IC_{50}) for IFNα2 (pg/ml); (B) residual viral replication (Vres) at the highest (5.5 pg/ml) IFNα2 dose (Vres); (*C*) Half-maximal inhibitory concentrations (IC_{50}) for IFNβ (pg/ml); (*D*) residual viral replication (Vres) at the highest (0.44 pg) IFNβ dose. Each dot represents an individual isolate derived from donor plasma (PL, green), donor genital secretions (CVL or SEM, purple), or recipient plasma (PL, red). Black lines denote the geometric mean, and fold changes are listed above groups when significant ($P < 0.05$). Orange dots indicating IFNα2 and IFNβ IC_{50} and Vres values for two available (CH040 and CH162) TF virus infectious molecular clones (4, 12) are shown for control.

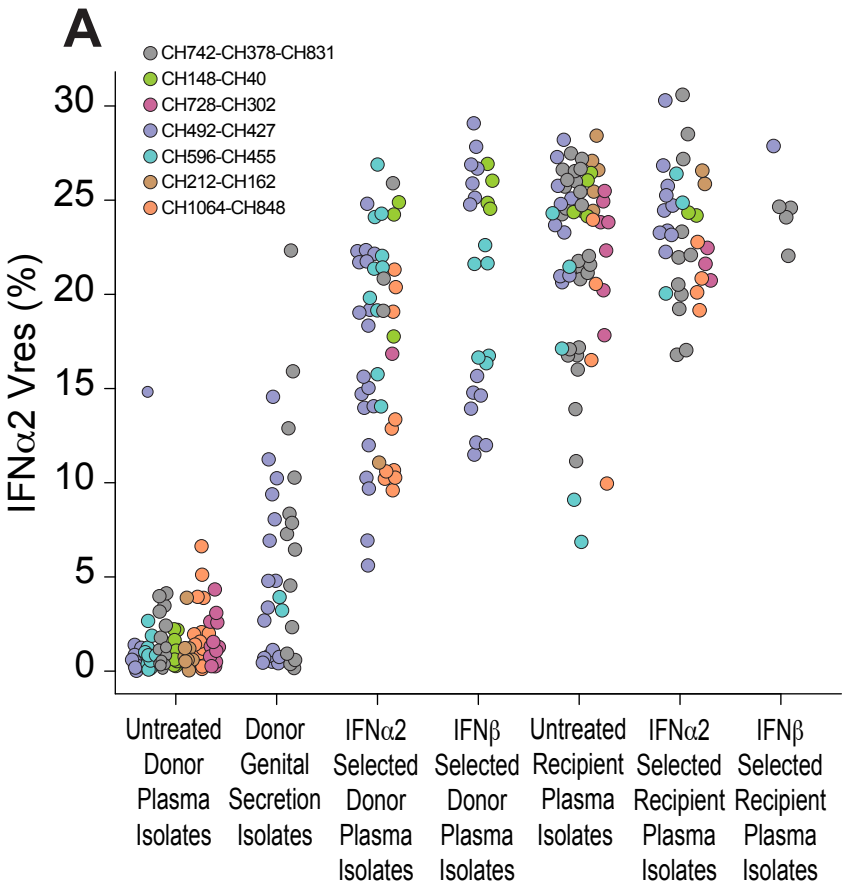

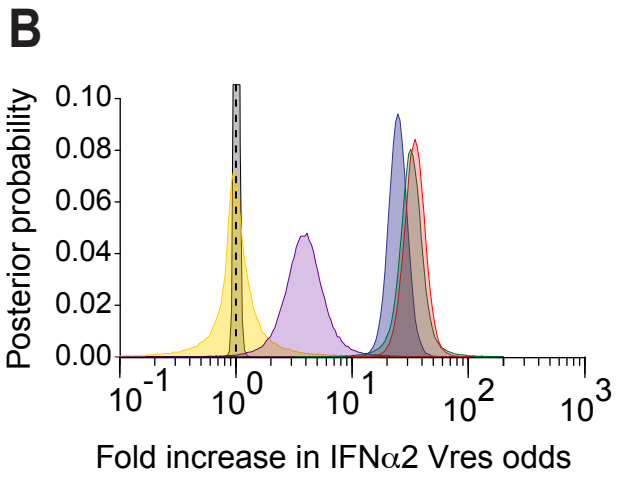

Untreated Donor Plasma Isolates vs	Fold	p (effect<1)
IFNα2–Selected Donor Isolates	24.7	<0.00001
IFNβ–Selected Donor Isolates	32.1	0.0002
Donor Genital Secretion Isolates	3.9	0.008
Untreated Recipient Plasma Isolates	34.6	<0.00001
Untreated Recipient Plasma Isolates vs		
IFNα2–Selected Recipient Isolates	1.0	0.37
IFNβ–Selected Recipient Isolates	1.0	0.51

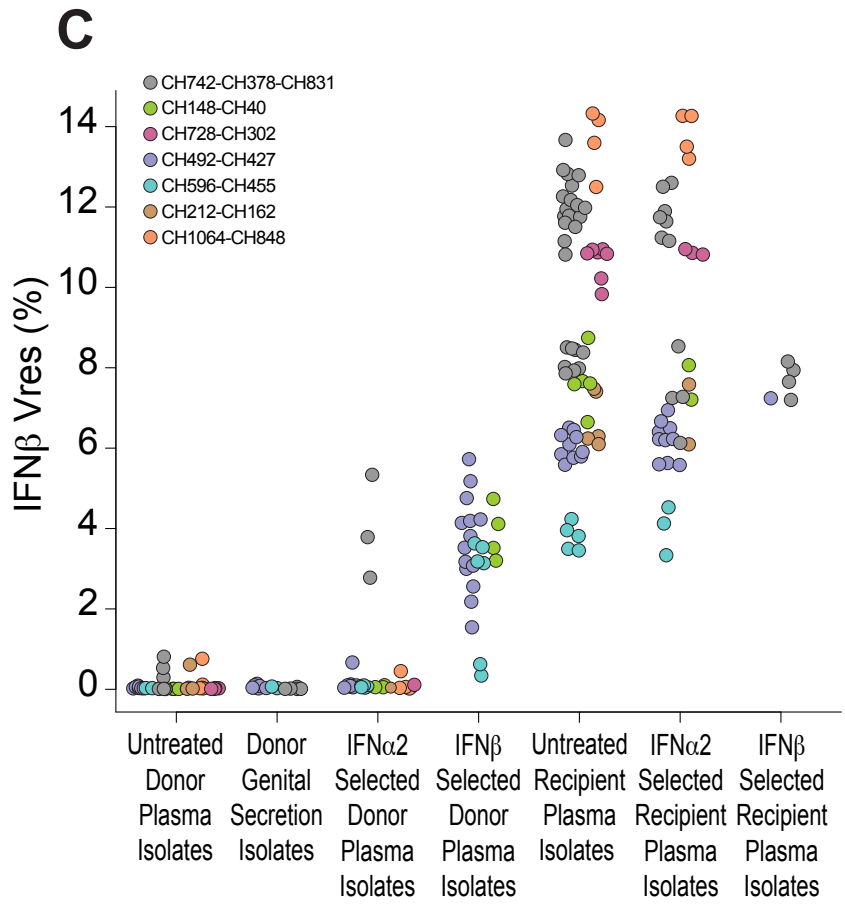

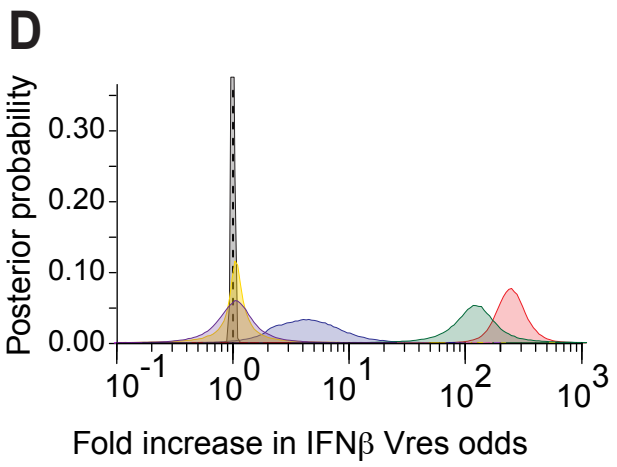

Untreated Donor Plasma Isolates vs	Fold	p (effect<1)
IFNα2–Selected Donor Isolates	4.4	0.02
IFNβ–Selected Donor Isolates	121.0	0.0002
Donor Genital Secretion Isolates	1.0	0.45
Untreated Recipient Plasma Isolates	250.3	<0.00001
Untreated Recipient Plasma Isolates vs		
IFNα2–Selected Recipient Isolates	1.0	0.59
IFNβ–Selected Recipient Isolates	1.1	0.37

Fig. S6. **Residual viral replication (Vres) of untreated and IFN-selected isolates from matched donor and recipient pairs.** (*A, C*) Donor and recipient isolates were tested for their ability to replicate in CD4+ T cells in the presence of maximal doses of IFNα2 (*A*) and IFNβ (*C*), expressed as the percentage of viral growth retained relative to growth in the absence of IFN. Viruses are colored by transmission pair and include untreated as well as IFNα2-selected and IFNβ-selected isolates from both donors and recipients. *(B, D*) A hierarchical Bayesian regression model was used to estimate the population-wide fold change in the odds of retaining replication in the presence of maximal (non-toxic) doses of IFNα2 (*B*) or IFNβ (*D*), when comparing untreated and IFNα2-selected donor plasma isolates (blue), untreated and IFNβ-selected donor plasma isolates (green), untreated donor plasma and genital secretion isolates (purple), untreated donor and recipient plasma isolates (red), untreated and IFNα2-selected recipient plasma isolates (grey) and untreated and IFNβ-selected recipient plasma isolates (yellow). The dashed vertical line marks a fold change of 1, indicating no effect. The estimated posterior probability distribution for each parameter is shown along with a table summarizing the expected fold change, and the probability that the effect is less than 1.

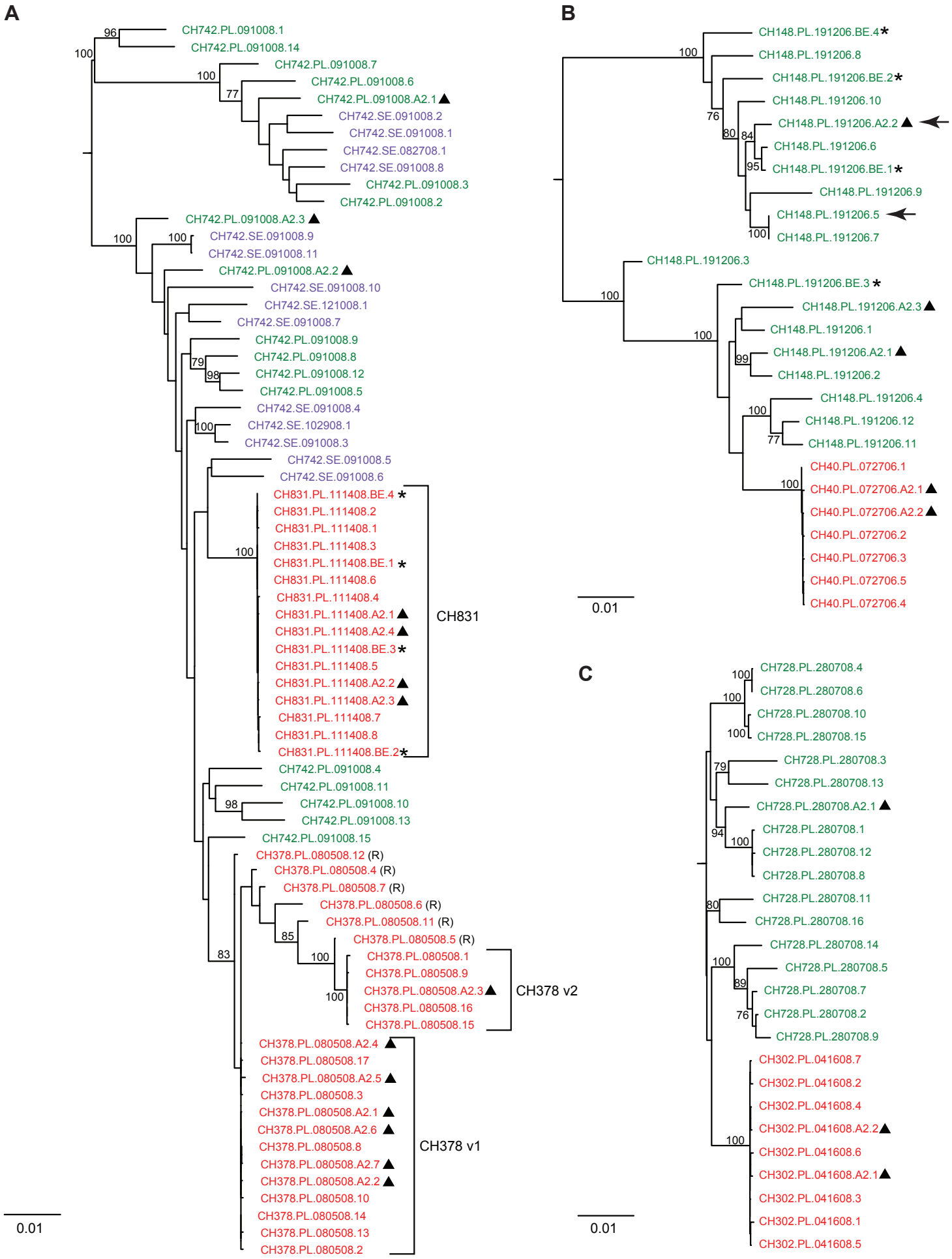
A
CH742.PL.091008.1
CH742.PL.091008.14
CH742.PL.091008.7
CH742.PL.091008.6
CH742.PL.091008.A2.1
CH742.SE.091008.2
CH742.SE.091008.1
CH742.SE.082708.1
CH742.SE.091008.8
CH742.PL.091008.3
CH742.PL.091008.2
CH742.PL.091008.A2.3
CH742.SE.091008.9
CH742.SE.091008.11
CH742.PL.091008.A2.2
CH742.SE.091008.10
CH742.SE.121008.1
CH742.SE.091008.7
CH742.PL.091008.9
CH742.PL.091008.8
CH742.PL.091008.12
CH742.PL.091008.5
CH742.SE.091008.4
CH742.SE.102908.1
CH742.SE.091008.3
CH742.SE.091008.5
CH742.SE.091008.6
CH831.PL.111408.BE.4 *
CH831.PL.111408.2
CH831.PL.111408.1
CH831.PL.111408.3
CH831.PL.111408.BE.1 *
CH831.PL.111408.6
CH831.PL.111408.4
CH831.PL.111408.A2.1
CH831.PL.111408.A2.4
CH831.PL.111408.BE.3 *
CH831.PL.111408.5
CH831.PL.111408.A2.2
CH831.PL.111408.A2.3
CH831.PL.111408.7
CH831.PL.111408.8
CH831.PL.111408.BE.2 *
CH831
CH742.PL.091008.4
CH742.PL.091008.11
CH742.PL.091008.10
CH742.PL.091008.13
CH742.PL.091008.15
CH378.PL.080508.12 (R)
CH378.PL.080508.4 (R)
CH378.PL.080508.7 (R)
CH378.PL.080508.6 (R)
CH378.PL.080508.11 (R)
CH378.PL.080508.5 (R)
CH378.PL.080508.1
CH378.PL.080508.9
CH378.PL.080508.A2.3
CH378.PL.080508.16
CH378.PL.080508.15
CH378 v2
CH378.PL.080508.A2.4
CH378.PL.080508.17
CH378.PL.080508.A2.5
CH378.PL.080508.3
CH378.PL.080508.A2.1
CH378.PL.080508.A2.6
CH378.PL.080508.8
CH378.PL.080508.A2.7
CH378.PL.080508.A2.2
CH378.PL.080508.10
CH378.PL.080508.14
CH378.PL.080508.13
CH378.PL.080508.2
CH378 v1
0.01
B
CH148.PL.191206.BE.4 *
CH148.PL.191206.8
CH148.PL.191206.BE.2 *
CH148.PL.191206.10
CH148.PL.191206.A2.2
CH148.PL.191206.6
CH148.PL.191206.BE.1 *
CH148.PL.191206.9
CH148.PL.191206.5
CH148.PL.191206.7
CH148.PL.191206.3
CH148.PL.191206.BE.3 *
CH148.PL.191206.A2.3
CH148.PL.191206.1
CH148.PL.191206.A2.1
CH148.PL.191206.2
CH148.PL.191206.4
CH148.PL.191206.12
CH148.PL.191206.11
CH40.PL.072706.1
CH40.PL.072706.A2.1
CH40.PL.072706.A2.2
CH40.PL.072706.2
CH40.PL.072706.3
CH40.PL.072706.5
CH40.PL.072706.4
0.01
C
CH728.PL.280708.4
CH728.PL.280708.6
CH728.PL.280708.10
CH728.PL.280708.15
CH728.PL.280708.3
CH728.PL.280708.13
CH728.PL.280708.A2.1
CH728.PL.280708.1
CH728.PL.280708.12
CH728.PL.280708.8
CH728.PL.280708.11
CH728.PL.280708.16
CH728.PL.280708.14
CH728.PL.280708.5
CH728.PL.280708.7
CH728.PL.280708.2
CH728.PL.280708.9
CH302.PL.041608.7
CH302.PL.041608.2
CH302.PL.041608.4
CH302.PL.041608.A2.2
CH302.PL.041608.6
CH302.PL.041608.A2.1
CH302.PL.041608.3
CH302.PL.041608.1
CH302.PL.041608.5
0.01

D

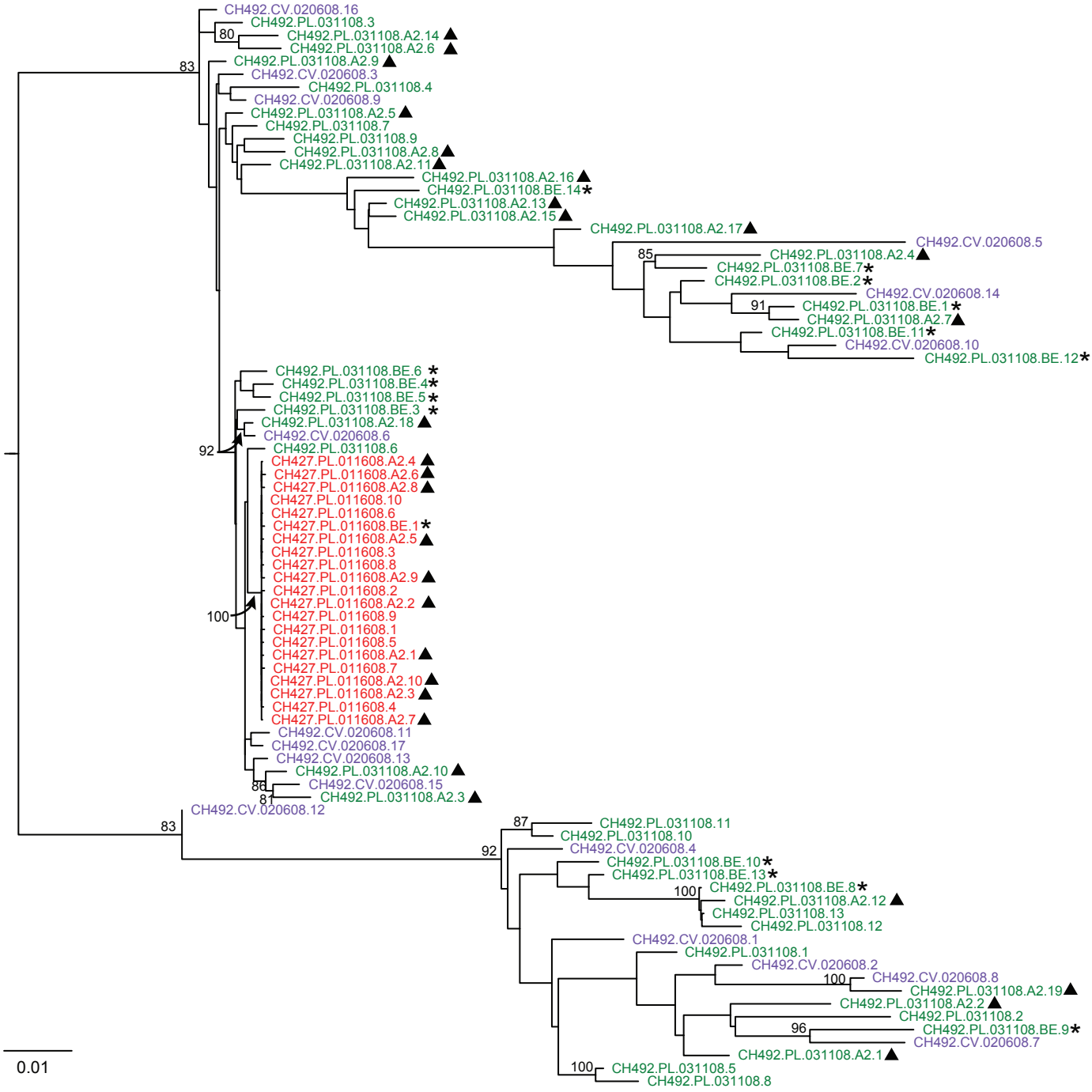
CH492.CV.020608.16
CH492.PL.031108.3
80
CH492.PL.031108.A2.14
CH492.PL.031108.A2.6
83
CH492.PL.031108.A2.9
CH492.CV.020608.3
CH492.PL.031108.4
CH492.CV.020608.9
CH492.PL.031108.A2.5
CH492.PL.031108.7
CH492.PL.031108.9
CH492.PL.031108.A2.8
CH492.PL.031108.A2.11
CH492.PL.031108.A2.16
CH492.PL.031108.BE.14*
CH492.PL.031108.A2.13
CH492.PL.031108.A2.15
CH492.PL.031108.A2.17
CH492.CV.020608.5
85
CH492.PL.031108.A2.4
CH492.PL.031108.BE.7*
CH492.PL.031108.BE.2*
CH492.CV.020608.14
91
CH492.PL.031108.BE.1*
CH492.PL.031108.A2.7
CH492.PL.031108.BE.11*
CH492.CV.020608.10
CH492.PL.031108.BE.12*
CH492.PL.031108.BE.6*
CH492.PL.031108.BE.4*
CH492.PL.031108.BE.5*
CH492.PL.031108.BE.3*
CH492.PL.031108.A2.18
CH492.CV.020608.6
92
CH492.PL.031108.6
CH427.PL.011608.A2.4
CH427.PL.011608.A2.6
CH427.PL.011608.A2.8
CH427.PL.011608.10
CH427.PL.011608.6
CH427.PL.011608.BE.1*
CH427.PL.011608.A2.5
CH427.PL.011608.3
CH427.PL.011608.8
CH427.PL.011608.A2.9
CH427.PL.011608.2
CH427.PL.011608.A2.2
100
CH427.PL.011608.9
CH427.PL.011608.1
CH427.PL.011608.5
CH427.PL.011608.A2.1
CH427.PL.011608.7
CH427.PL.011608.A2.10
CH427.PL.011608.A2.3
CH427.PL.011608.4
CH427.PL.011608.A2.7
CH492.CV.020608.11
CH492.CV.020608.17
CH492.CV.020608.13
CH492.PL.031108.A2.10
86
CH492.CV.020608.15
81
CH492.PL.031108.A2.3
CH492.CV.020608.12
83
87
CH492.PL.031108.11
CH492.PL.031108.10
92
CH492.CV.020608.4
CH492.PL.031108.BE.10*
CH492.PL.031108.BE.13*
100
CH492.PL.031108.BE.8*
CH492.PL.031108.A2.12
CH492.PL.031108.13
CH492.PL.031108.12
CH492.CV.020608.1
CH492.PL.031108.1
CH492.CV.020608.2
100
CH492.CV.020608.8
CH492.PL.031108.A2.19
CH492.PL.031108.A2.2
CH492.PL.031108.2
96
CH492.PL.031108.BE.9*
CH492.CV.020608.7
CH492.PL.031108.A2.1
100
CH492.PL.031108.5
CH492.PL.031108.8
0.01

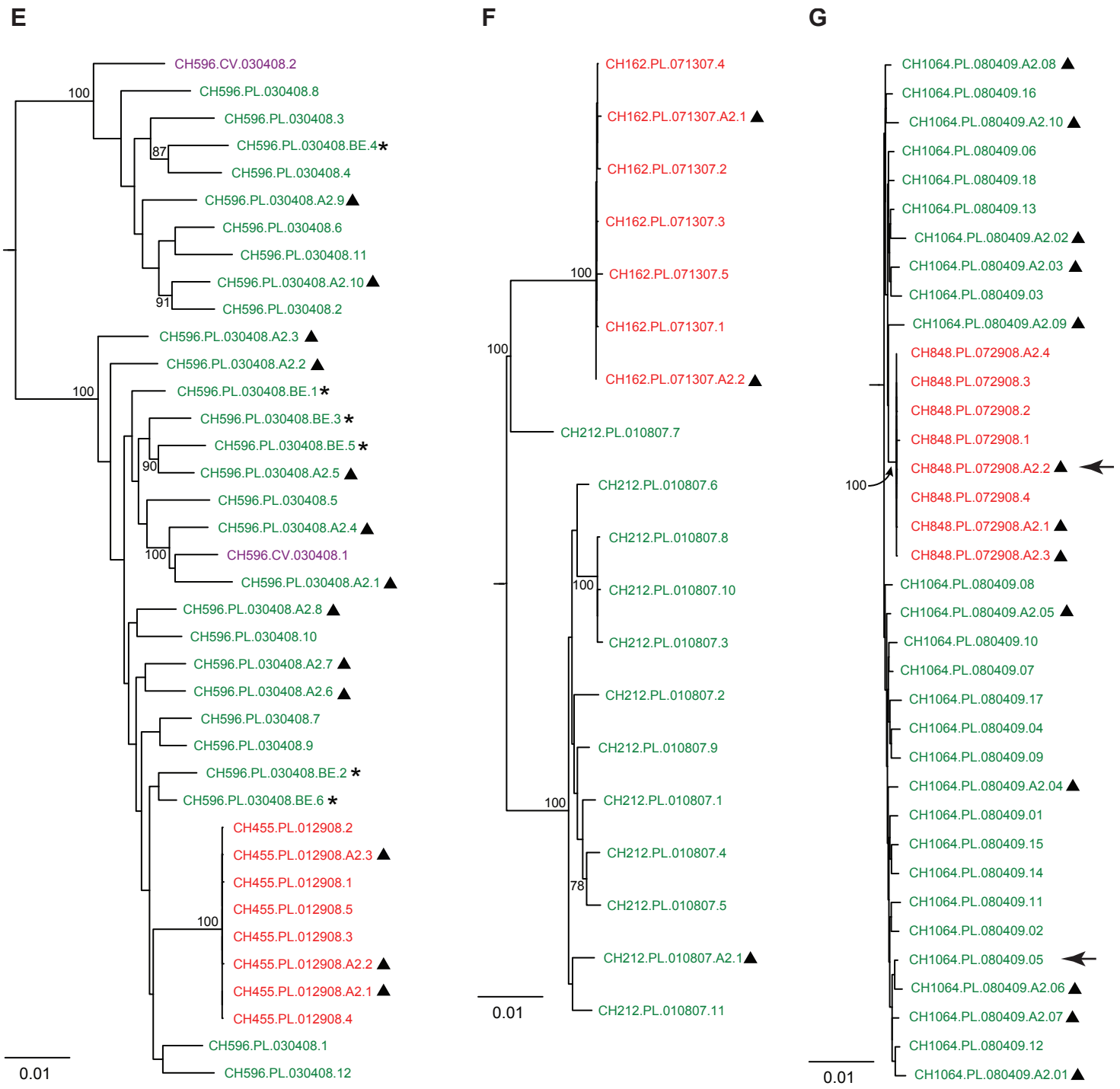
E
CH596.CV.030408.2
CH596.PL.030408.8
CH596.PL.030408.3
CH596.PL.030408.BE.4*
CH596.PL.030408.4
CH596.PL.030408.A2.9▲
CH596.PL.030408.6
CH596.PL.030408.11
CH596.PL.030408.A2.10▲
CH596.PL.030408.2
CH596.PL.030408.A2.3▲
CH596.PL.030408.A2.2▲
CH596.PL.030408.BE.1*
CH596.PL.030408.BE.3*
CH596.PL.030408.BE.5*
CH596.PL.030408.A2.5▲
CH596.PL.030408.5
CH596.PL.030408.A2.4▲
CH596.CV.030408.1
CH596.PL.030408.A2.1▲
CH596.PL.030408.A2.8▲
CH596.PL.030408.10
CH596.PL.030408.A2.7▲
CH596.PL.030408.A2.6▲
CH596.PL.030408.7
CH596.PL.030408.9
CH596.PL.030408.BE.2*
CH596.PL.030408.BE.6*
CH455.PL.012908.2
CH455.PL.012908.A2.3▲
CH455.PL.012908.1
CH455.PL.012908.5
CH455.PL.012908.3
CH455.PL.012908.A2.2▲
CH455.PL.012908.A2.1▲
CH455.PL.012908.4
CH596.PL.030408.1
CH596.PL.030408.12
100
87
91
100
90
100
100
0.01
F
CH162.PL.071307.4
CH162.PL.071307.A2.1▲
CH162.PL.071307.2
CH162.PL.071307.3
CH162.PL.071307.5
CH162.PL.071307.1
CH162.PL.071307.A2.2▲
CH212.PL.010807.7
CH212.PL.010807.6
CH212.PL.010807.8
CH212.PL.010807.10
CH212.PL.010807.3
CH212.PL.010807.2
CH212.PL.010807.9
CH212.PL.010807.1
CH212.PL.010807.4
CH212.PL.010807.5
CH212.PL.010807.A2.1▲
CH212.PL.010807.11
100
100
100
100
78
0.01
G
CH1064.PL.080409.A2.08▲
CH1064.PL.080409.16
CH1064.PL.080409.A2.10▲
CH1064.PL.080409.06
CH1064.PL.080409.18
CH1064.PL.080409.13
CH1064.PL.080409.A2.02▲
CH1064.PL.080409.A2.03▲
CH1064.PL.080409.03
CH1064.PL.080409.A2.09▲
CH848.PL.072908.A2.4
CH848.PL.072908.3
CH848.PL.072908.2
CH848.PL.072908.1
CH848.PL.072908.A2.2▲
CH848.PL.072908.4
CH848.PL.072908.A2.1▲
CH848.PL.072908.A2.3▲
CH1064.PL.080409.08
CH1064.PL.080409.A2.05▲
CH1064.PL.080409.10
CH1064.PL.080409.07
CH1064.PL.080409.17
CH1064.PL.080409.04
CH1064.PL.080409.09
CH1064.PL.080409.A2.04▲
CH1064.PL.080409.01
CH1064.PL.080409.15
CH1064.PL.080409.14
CH1064.PL.080409.11
CH1064.PL.080409.02
CH1064.PL.080409.05
CH1064.PL.080409.A2.06▲
CH1064.PL.080409.A2.07▲
CH1064.PL.080409.12
CH1064.PL.080409.A2.01▲
100
0.01

Fig. S7. Phylogenetic relationships of IFN-selected and unselected isolates from matched donor and recipient pairs. Nucleotide sequences were aligned using CLUSTALW v. 2 (16), with ambiguous regions removed. Maximum likelihood trees with bootstrap support (1,000 replicates) were constructed using PhyML v. 3.1 (17) with evolutionary models selected using jModelTest v. 2.1.4 (19). Donor plasma isolate sequences (labeled PL, followed by the date and the isolate number) and genital tract isolate sequences (labeled SE for semen and CV for cervicovaginal lavage, followed by the date and isolate number) are shown in green and purple, respectively, while recipient plasma isolate sequences are shown in red (labeled PL, followed by the date and the isolate number). Isolates obtained in CD4+ T cells pretreated with IFNα2 (A2) or IFNβ (BE) are highlighted by asterisks and triangles, respectively. Bootstrap values ≥ 75% are shown (scale bars represent 0.01 substitutions per site). (*A*) Phylogenetic tree of near complete isolate sequences (8,812 bp) from donor CH742 and recipients CH831 and CH378 (denoted by brackets). CH378 was infected by two TF viruses (v1 and v2; recombinants of v1 and v2 are indicated with an "R"). (*B*) Phylogenetic tree of near complete isolate sequences (8,737 bp) from donor CH148 and recipient CH040; (*C*) Phylogenetic tree of near complete isolate sequences (8,872 bp) from donor CH728 and recipient CH302; (*D*) Phylogenetic tree of near complete isolate sequences (8,582 bp) from donor CH492 and recipient CH427; (*E*) Phylogenetic tree of near complete isolate sequences (8,674 bp) from donor CH596 and recipient CH455; (*F*) Phylogenetic tree of near complete isolate sequences (8,795 bp) from donor CH212 and recipient CH162; (*G*) Phylogenetic tree of near complete isolate sequences (8,861 bp) from donor CH1064 and recipient CH848. Arrows indicate examples of isolates with identical *vpu* sequences that differed in their p24 release capacity.